Eur. Phys. J. A **1**, 99–114 (1998)

THE EUROPEAN PHYSICAL JOURNAL A

Subthreshold K^+ meson production in proton–nucleus reactions and nucleon spectral function

S.V. Efremov[1], E.Ya. Paryev[2]

[1] Bonner Nuclear Laboratory, Rice University, P.O. Box 1892, Houston, TX 77005-1892, USA
[2] Institute for Nuclear Research, Russian Academy of Sciences, Moscow 117312, Russia

Received: 2 April 1997 / Revised version: 7 August 1997

Abstract. The inclusive K^+ meson production in proton–nucleus collisions in the near threshold and subthreshold energy regimes is analyzed with respect to the one–step ($pN \to K^+YN, Y = \Lambda, \Sigma$) and two–step ($pN \to NN\pi, NN2\pi$; $\pi N \to K^+Y$) incoherent production processes on the basis of an appropriate new folding model, which takes properly into account the struck target nucleon removal energy and momentum distribution (nucleon spectral function), extracted from recent quasielastic electron scattering experiments and from many–body calculations with realistic models of the NN interaction. Comparison of the model calculations of the K^+ total and double differential cross sections for the reaction $p + C^{12}$ with the existing experimental data is given, illustrating both the relative role of the primary and secondary production channels at considered incident energies and those features of the cross sections which are sensitive to the high momentum and high removal energy part of the nucleon spectral function that is governed by nucleon–nucleon short–range and tensor correlations. It is found that the in–medium modifications of the available for pion and kaon production invariant energies squared due to the respective optical potentials are needed to account for considered experimental data.

PACS. 25.40.-k Nucleon induced reactions

Introduction

An extensive investigations of the production of K^+ mesons in proton–nucleus reactions [1–9] at incident energies lower than the free nucleon-nucleon threshold have been carried out in the last years. The study of inclusive and exclusive subthreshold K^+ production in pA interactions is planned in the near future at the accelerators COSY–Jülich [10] and CELSIUS [11]. Because of the high K^+ production threshold ($1.58\ GeV$) in the nucleon-nucleon collision and the rather weak K^+ rescattering in the surrounding medium compared to the pions, etas, antiprotons and antikaons, from these studies one hopes to extract information about both the intrinsic properties of target nuclei (such as Fermi motion, high momentum components of the nuclear wave function, clusters of nucleons or quarks) and reaction mechanism, in–medium properties of hadrons. However, in spite of large efforts, subthreshold kaon production in proton–nucleus reactions is still far from being fully understood. Thus, measured total K^+ production cross sections [1] in the range of proton energies of 800–1000 MeV were described in the framework of the respective folding models based on both the direct mechanism [2,6] of K^+ production ($pN \to K^+\Lambda N$) and on the two–step mechanism [3–5] associated with the production of kaons by intermediate pions ($pN_1 \to \pi NN$, $\pi N_2 \to K^+\Lambda$) using different parametrizations for internal nucleon momentum distribution [6, 12, 13]. The same experimental data could be well explained also in the modified phase space model [7]. In the above folding models only the internal nucleon momentum distribution has been used and the off–shell propagation of the struck target nucleon has been neglected or has been taken into account the most crudely, but it could be significant in processes that are limited by phase space such as the threshold heavy meson production. As is well known [13–21], the off–shell behaviour of a bound nucleon is described by the nucleon spectral function $P(\mathbf{p}_t, E)$, which represents the probability to find in the nucleus a nucleon with momentum $\mathbf{p}_t$ and removal (binding) energy E and contains all the information on the structure of a target nucleus. The knowledge of the spectral function $P(\mathbf{p}_t, E)$ is needed for calculations of cross sections of various kinds of nuclear reactions. In particular, it has been widely used earlier for the analysis of inclusive and exclusive quasielastic electron scattering by nuclei [13–27]. It was found that even at very high momentum and energy transfer in this scattering, the target nucleus cannot be simply described as a collection of A on–shell nucleons subject only to Fermi motion, but the full nucleon momentum and binding energy distribution has to be considered. Only recently [8, 9, 28] the binding energy of the struck target nucleon

has been properly taken into account in calculating the subthreshold kaon production in pA collisions. Debowski et al. [8] analyzed their own measured double differential cross sections for the K^+ production in $p+C$ reactions at 1.2, 1.5 and 2.5 GeV beam energies and in $p+Pb$ collisions at 1.2 and 1.5 GeV in the framework of the advanced binary collision model based on free elementary cross sections for particle production and on the nucleon spectral function taken from [20, 27]. It was shown that at subthreshold incident energies the measured total [1] and differential [8] K^+ production cross sections are underestimated significantly by calculations assuming only first chance collisions. When secondary kaon production processes have been taken into account, the results of calculations for the double differential cross sections for K^+ production from pC and pPb reactions are in much better agreement with the experimental data. The same nucleon spectral function has been employed by Sibirtsev et al. [9] for the description of the measured [1] total cross sections for K^+ production from $p+C$ collisions in the framework of the two–step model. The claims have been advanced in [9] that within the spectral function approach the two–step production mechanism with an intermediate pion also dominates at subthreshold energies as in the folding models [3–5], but the calculated total cross sections for K^+ production are underestimated below about 920 MeV in contrast to the folding model where a better description of the experimental data is achieved as well as the contribution to the calculated total cross sections from the high momentum and high removal energy part (correlated part) of the nucleon spectral function is small compared to that calculated with the single–particle (uncorrelated) part of the one. However, in order to fully clarify the role played by nucleon–nucleon correlations induced by realistic interactions in the subthreshold kaon production in pA collisions as well as to get a deeper insight into the relative role of the primary and secondary reaction channels, it is obviously necessary to properly analyze within the same approach, based on nucleon spectral function, the existing experimental data both on total [1] and differential [8] kaon production cross sections.

In this study we have performed such analysis of the total and differential K^+ production cross sections from pC reactions in the near threshold and subthreshold energy regimes using the appropriate new folding model for primary and secondary production processes, which takes into account the struck target nucleon removal energy and momentum distribution. Some preliminary results of this study have been reported in [28].

1 Direct K^+ production processes

1.1 Kaon production cross section

Apart from participation in the elastic scattering an incident proton can produce a K^+ directly in the first inelastic pN collision due to nucleon Fermi motion. Since we are interested in a few GeV region (up to 2.5 GeV), we have taken into account [29] the following elementary processes which have the lowest free production thresholds:

$$p+N \to K^+ + \Lambda + N, \tag{1}$$

$$p+N \to K^+ + \Sigma + N. \tag{2}$$

Because the kaon final–state interactions (propagation in the mean–field potential and kaon–nucleon elastic scattering) modify the kaon momentum spectrum mainly at large laboratory angles ($> 45^0$) [30–34] and since we have an intention to calculate the kaon spectrum at an angle of 40^0, where the cross section is measured [8], we will neglect the kaon final–state interactions in the present study[1]. Moreover, since the kaon production thresholds in the medium for the elementary processes under consideration are not affected by medium effects [37], we will also ignore the medium modification of hadron masses in the present work. Then we can represent the invariant inclusive cross section of K^+ production on nuclei by the initial proton with momentum $\mathbf{p}_0$ as follows [13, 23, 38]:

$$E_{K^+}\frac{d\sigma^{(prim)}_{pA\to K^+X}(\mathbf{p}_0)}{d\mathbf{p}_{K^+}} = I_V[A]\times \left\{\left\langle E_{K^+}\frac{d\sigma_{pN\to K^+\Lambda N}(\mathbf{p}_0,\mathbf{p}_{K^+})}{d\mathbf{p}_{K^+}}\right\rangle + \left\langle E_{K^+}\frac{d\sigma_{pN\to K^+\Sigma N}(\mathbf{p}_0,\mathbf{p}_{K^+})}{d\mathbf{p}_{K^+}}\right\rangle\right\}, \tag{3}$$

where

$$I_V[A] = A\int \rho(\mathbf{r})d\mathbf{r}\exp\left[-\mu(p_0)\int\limits_{-\infty}^{0}\rho(\mathbf{r}+x\boldsymbol{\Omega}_0)dx\right], \tag{4}$$

$$\mu(p_0) = \sigma^{in}_{pp}(p_0)Z + \sigma^{in}_{pn}(p_0)N; \tag{5}$$

$$\left\langle E_{K^+}\frac{d\sigma_{pN\to K^+YN}(\mathbf{p}_0,\mathbf{p}_{K^+})}{d\mathbf{p}_{K^+}}\right\rangle = \iint P(\mathbf{p}_t,E)d\mathbf{p}_t dE\times \times\left[E_{K^+}\frac{d\sigma_{pN\to K^+YN}(\sqrt{s},\mathbf{p}_{K^+})}{d\mathbf{p}_{K^+}}\right]. \tag{6}$$

Here, $E_{K^+}d\sigma_{pN\to K^+YN}(\sqrt{s},\mathbf{p}_{K^+})/d\mathbf{p}_{K^+}$ are the free invariant inclusive cross sections for K^+ production in reactions (1), (2); $\rho(\mathbf{r})$ and $P(\mathbf{p}_t,E)$ are the density and nucleon spectral function normalized to unity; $\mathbf{p}_t$ and E are the internal momentum and removal energy of the struck target nucleon just before the collision; $\sigma^{in}_{pN}(p_0)$ is

[1] This is allowed in calculating the total kaon yield as kaons cannot be absorbed in nuclear medium due to the strangeness conservation. It should be, however, pointed out that current calculations based on such theoretical approaches as the effective chiral Lagrangian, the Nambu–Jona–Lasinio model and the impulse approximation with the KN scattering length give essentially different predictions for the kaon potential in a nuclear medium [35, 36]. The study of kaon production in proton–nucleus collisions at large laboratory angles as one may hope to shed light on the kaon potential in nuclear matter

Table 1. Parameters in the approximation of the partial cross sections for the production of K^+ mesons in pp–collisions

Reaction	A_Y,$\mu b \cdot GeV^{-2}$	B_Y, GeV^{-2}	C_Y,$\mu b \cdot GeV^{-2}$	s_{th},GeV^2
$p+p \rightarrow K^+ + \Lambda + p$	122.943	2.015	77750.	6.490
$p+p \rightarrow K^+ + \Sigma + N$	104.026	1.006	0.	6.880

the inelastic cross section of free pN interaction; Z and N are the numbers of protons and neutrons in the target nucleus (A=N+Z); $\boldsymbol{\Omega}_0 = \mathbf{p}_0/p_0$; $\mathbf{p}_{K^+}$ and E_{K^+} are the momentum and total energy of a K^+ meson, respectively; $E_{K^+} = \sqrt{p_{K^+}^2 + m_K^2}$ (m_K is the rest mass of a kaon in free space); s is the pN center–of–mass energy squared. The expression for s is:

$$s = (E_0 + E_t)^2 - (\mathbf{p}_0 + \mathbf{p}_t)^2, \tag{7}$$

where E_0 and E_t are the projectile's total energy, given by $E_0 = \sqrt{p_0^2 + m_N^2}$ (m_N is the rest mass of a nucleon), and the struck target nucleon total energy, respectively. Taking into account the recoil and excitation energies of the residual $(A-1)$ system, one has [23]:

$$E_t = M_A - \sqrt{(-\mathbf{p}_t)^2 + (M_A - m_N + E)^2}, \tag{8}$$

where M_A is the mass of the initial target nucleus. It is easily seen that in this case the struck target nucleon is off–shell. In (3) it is assumed that the K^+ meson production cross sections in pp– and pn–interactions are the same [8, 29] as well as it is disregarded any difference between the proton and the neutron spectral functions [18]. In our approach the invariant inclusive cross sections for K^+ production in the elementary processes (1), (2) have been described by the three–body phase space calculations normalized to the corresponding total cross sections [29]:

$$E_{K^+}\frac{d\sigma_{pN\rightarrow K^+YN}(\sqrt{s},\mathbf{p}_{K^+})}{d\mathbf{p}_{K^+}} = \frac{\pi}{4}\frac{\sigma_{pN\rightarrow K^+YN}(\sqrt{s})}{I_3(s,m_K,m_Y,m_N)}\frac{\lambda(s_{YN},m_Y^2,m_N^2)}{s_{YN}}, \tag{9}$$

$$I_3(s,m_K,m_Y,m_N) = (\frac{\pi}{2})^2 \int\limits_{(m_Y+m_N)^2}^{(\sqrt{s}-m_K)^2} \frac{\lambda(s_{YN},m_Y^2,m_N^2)}{s_{YN}}\frac{\lambda(s,s_{YN},m_K^2)}{s}\,ds_{YN}, \tag{10}$$

$$\lambda(x,y,z) = \sqrt{\left[x-(\sqrt{y}+\sqrt{z})^2\right]\left[x-(\sqrt{y}-\sqrt{z})^2\right]}, \tag{11}$$

$$s_{YN} = s + m_K^2 - 2(E_0+E_t)E_{K^+} + 2(\mathbf{p}_0+\mathbf{p}_t)\mathbf{p}_{K^+}. \tag{12}$$

Here, $\sigma_{pN\rightarrow K^+YN}$ are the total cross sections for K^+ production in reactions (1), (2); m_Y is the mass in free space of a Y hyperon (Λ or Σ). For the total cross sections $\sigma_{pN\rightarrow K^+YN}$ we have used the parametrization suggested in [29] that has been corrected[2] for the new data point for $pp \rightarrow K^+\Lambda p$ reaction from COSY [39] at beam momentum of 2.345 GeV/c, viz.:

$$\sigma_{pp\rightarrow K^+YN}(\sqrt{s}) = \frac{A_Y(s-s_{th})^2}{4m_p^2 + B_Y(s-s_{th})^2} + C_Y(s-s_{th})^2[0.5-(s-s_{th})/GeV^2]^{8.83} \times \Theta[0.5-(s-s_{th})/GeV^2]/(4m_p^2), \tag{13}$$

where $\Theta(x) = (x+|x|)/2|x|$ and the constants A_Y, B_Y, C_Y and s_{th} are given in Table 1. The comparison of the results of our calculations by (13) (long–dashed line) with the experimental data (dots) for $pp \rightarrow K^+\Lambda p$ reaction is shown in Figure 1. In this Figure we also show the predictions from widely used in pA and AA simulations linear parametrization [40] (short–dashed line) and quartic parametrization [41] (dot–dashed line) corrected for the isospin invariance of the strong interaction, which are given, respectively, by:

$$\sigma_{linear} = 24\frac{\overset{*}{p}_{max}}{m_K}[\mu\mathrm{b}],\ \sigma_{\mathrm{quartic}} = \frac{2}{3}800\left[\frac{\overset{*}{\mathrm{p}}_{\mathrm{max}}}{\mathrm{GeV/c}}\right]^4[\mu\mathrm{b}], \tag{14}$$

where

$$\overset{*}{p}_{max} = \frac{1}{2\sqrt{s}}\lambda(s,(m_N+m_\Lambda)^2,m_K^2). \tag{15}$$

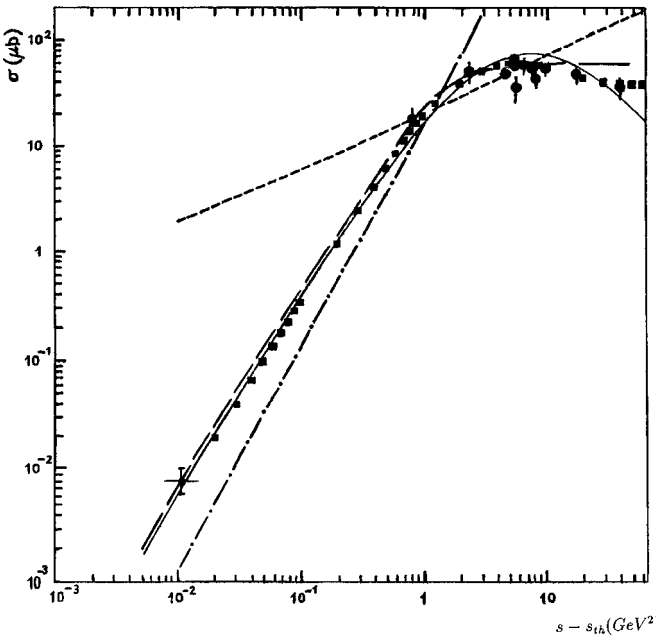

Fig. 1. The total cross section for $pp \rightarrow K^+\Lambda p$ reaction as a function of $s - s_{th}$ with s being the pp center–of–mass energy squared and $s_{th} = 6.490\ GeV^2$. The notations: see text

[2] It is interesting to note that such correction, as showed our calculations, leads to increase of the respective kaon production cross sections in pA collisions only by several percents at the kinetic energy ϵ_0 of a primary proton in lab system $\epsilon_0 \geq 1\ GeV$

The results from the boson exchange model [6] (squares), taking into account the one–pion and one–kaon exchange diagrams, as well as their parametrization (solid line) by the expression [6]

$$\sigma_{pp\to K^+\Lambda p}(\sqrt{s}) = 732.16(1-s_{th}/s)^{1.8}(s_{th}/s)^{1.5}[\mu\mathrm{b}] \quad (16)$$

are shown also in Fig. 1. It is seen that our parametrization (13) is close to the results from the boson exchange model at different energies, and is considerably smaller at low energies (in the vicinity of the lowest experimental point from COSY at $s - s_{th} = 0.0105\ GeV^2$) than the linear parametrization and larger than the quartic parametrization. Therefore, the use of the linear parametrization for the analysis of subthreshold kaon production in proton–nucleus and nucleus–nucleus interactions apparently overestimates the contribution from nucleon–nucleon collisions.

Consider now the integral (4) which represents the effective number of nucleons for the $pN \to K^+YN$ reaction on nuclei. A simpler expression can be given [38] for $I_V[A]$ in the case of Gaussian nuclear density ($\rho(\mathbf{r}) = (b/\pi)^{3/2}\exp(-br^2)$, $b = 0.248$ fm^{-2} for C^{12}):

$$I_V[A] = \frac{A}{x_G}\int\limits_0^1 \frac{dt}{t}(1-e^{-x_G t}), \quad x_G = \mu(p_0)b/\pi. \quad (17)$$

Numerical calculations, carried out in accordance with the formulas (5), (17) with taking into account that $\sigma_{pN}^{in} \approx 30$ mb [29] in the proton energy range of interest, show that for C^{12} target nucleus the effective number of nucleons is equal to 6.9. It should be noted that this value of the effective number of nucleons agrees well with the scaling factor of 7 used in [8] for the number of first chance proton–nucleon collisions in the case of C^{12} target nucleus.

1.2 Nucleon spectral function and internal nucleon momentum distribution

The nucleon spectral function, $P(\mathbf{p}_t, E)$, is a crucial point in the evaluation of the subthreshold production of any particles on a nuclear target. When ground–state NN correlations, which are generated by the short range and tensor parts of realistic NN interaction, are considered, the spectral function $P(\mathbf{p}_t, E)$ can be represented in the following form [16–21]:

$$P(\mathbf{p}_t, E) = P_0(\mathbf{p}_t, E) + P_1(\mathbf{p}_t, E), \quad (18)$$

where P_0 includes the ground and one–hole states of the residual $(A-1)$ nucleon system and P_1 more complex configurations (mainly 1p–2h states) that arise from 2p–2h excited states generated in the ground state of the target nucleus by NN correlations. Before considering the specific expressions for functions P_0 and P_1, let us recall several important quantities which are related to the nucleon spectral function, namely [16, 21]: the internal nucleon momentum distribution

$$\begin{aligned} n(\mathbf{p}_t) &= \int P(\mathbf{p}_t, E)dE \quad (19)\\ &= \int P_0(\mathbf{p}_t, E)dE + \int P_1(\mathbf{p}_t, E)dE \\ &= n_0(\mathbf{p}_t) + n_1(\mathbf{p}_t), \end{aligned}$$

the mean nucleon kinetic energy

$$< T >= \iint \frac{p_t^2}{2m_N} P(\mathbf{p}_t, E)d\mathbf{p}_t dE = \int \frac{p_t^2}{2m_N} n(\mathbf{p}_t)d\mathbf{p}_t, \quad (20)$$

and the mean nucleon removal energy

$$< E >= \iint EP(\mathbf{p}_t, E)d\mathbf{p}_t dE. \quad (21)$$

The last two quantities are related to the total binding energy per nucleon ϵ_A by the following energy sum rule (the Koltun sum rule [42]):

$$\epsilon_A = \frac{1}{2}\left(\frac{A-2}{A-1} < T > - < E >\right), \quad (22)$$

if the nuclear hamiltonian contains only two–body density independent forces. The quantities ϵ_A and $n(\mathbf{p}_t)$ have been calculated [16, 17, 21, 43] for different nuclear systems ranging from light nuclei to infinite nuclear matter within the framework of many–body approaches with realistic NN interactions, so that the theoretical values of $< T >$ and $< E >$ for various nuclei are known presently [16, 21].

Disregarding the finite width of the states below the Fermi level[3], the spectral function $P_0(\mathbf{p}_t, E)$ can be represented in the following form [16–19, 21]:

$$P_0(\mathbf{p}_t, E) = \frac{1}{A}\sum_\alpha A_\alpha n_\alpha(\mathbf{p}_t)\delta(E - |\epsilon_\alpha|), \quad (23)$$

where $n_\alpha(\mathbf{p}_t)$ is the nucleon momentum distribution of the single–particle state α having energy ϵ_α and number of nucleons A_α ($\sum_\alpha A_\alpha = A$), the sum over α runs only over the states below the Fermi sea. In the absence of NN correlations (within the mean–field approximation) function $P_1(\mathbf{p}_t, E) = 0$, momentum distribution $n_\alpha(\mathbf{p}_t)$ reduces to the mean–field momentum distribution $n_\alpha^{(MF)}(\mathbf{p}_t)$ and the mean–field nucleon spectral function is recovered [16–21], viz.:

$$P_0^{(MF)}(\mathbf{p}_t, E) = \frac{1}{A}\sum_\alpha A_\alpha n_\alpha^{(MF)}(\mathbf{p}_t)\delta(E - |\epsilon_\alpha|). \quad (24)$$

The normalization (spectroscopic factors or occupation probabilities) of $n_\alpha^{(MF)}(\mathbf{p}_t)$ and $n_\alpha(\mathbf{p}_t)$ are different, namely:

$$\begin{aligned} S_\alpha^{(MF)} &= \int n_\alpha^{(MF)}(\mathbf{p}_t)d\mathbf{p}_t = 1, \quad (25)\\ S_\alpha &= \int n_\alpha(\mathbf{p}_t)d\mathbf{p}_t < 1. \end{aligned}$$

[3] Such approximation is allowed in calculating the inclusive cross sections [18] we are interested in

Thus, the NN correlations deplete ($20 \pm 5\%$, [16, 17, 21, 26, 44], i.e. $S_\alpha = S_0 = 0.8$) states below the Fermi sea and populate states outside the Fermi sea. Therefore, the following normalizations for the spectral functions $P_0(\mathbf{p}_t, E)$ and $P_1(\mathbf{p}_t, E)$ as well as for the momentum distributions $n_0(\mathbf{p}_t)$ and $n_1(\mathbf{p}_t)$ hold:

$$\int\int P_0(\mathbf{p}_t, E) d\mathbf{p}_t dE = \int n_0(\mathbf{p}_t) d\mathbf{p}_t = S_0 = 0.8, \quad (26)$$

$$\int\int P_1(\mathbf{p}_t, E) d\mathbf{p}_t dE = \int n_1(\mathbf{p}_t) d\mathbf{p}_t = S_1 = 1 - S_0 = 0.2. \quad (27)$$

For K^+ production calculations in the case of C^{12} target nucleus reported here, taking into account that the main difference between $n_\alpha(\mathbf{p}_t)$ and $n_\alpha^{(MF)}(\mathbf{p}_t)$ concerns their normalization [16–18], we have employed for the single–particle part $P_0(\mathbf{p}_t, E)$ of the nucleon spectral function the following relation:

$$P_0(\mathbf{p}_t, E) = S_0 P_0^{(MF)}(\mathbf{p}_t, E) \quad (28)$$

with $P_0^{(MF)}(\mathbf{p}_t, E)$ being the harmonic oscillator spectral function (see, e.g., [24]):

$$P_0^{(MF)}(\mathbf{p}_t, E) = \frac{4}{A} n_{1s}(\mathbf{p}_t) \delta(E - |\epsilon_{1s}|) + \left(\frac{A-4}{A}\right) n_{1p}(\mathbf{p}_t) \delta(E - |\epsilon_{1p}|) \quad (29)$$

in which the s– and p–shell nucleon momentum distributions $n_{1s}(\mathbf{p}_t)$ and $n_{1p}(\mathbf{p}_t)$ were taken from [38]:

$$n_{1s}(\mathbf{p}_t) = (b_0/\pi)^{3/2} \exp(-b_0 p_t^2), \quad (30)$$
$$n_{1p}(\mathbf{p}_t) = \frac{2}{3}(b_0/\pi)^{3/2} b_0 p_t^2 \exp(-b_0 p_t^2)$$

($b_0 = 68.5(\mathrm{GeV/c})^{-2}$) and binding energies of $|\epsilon_{1s}| = 34$ and $|\epsilon_{1p}| = 16\ MeV$ [24] for the s and p shells, respectively, were used. Within the representation (28), the single–particle part $n_0(\mathbf{p}_t)$ of the nucleon momentum distribution becomes:

$$n_0(\mathbf{p}_t) = \frac{S_0 (b_0/\pi)^{3/2}}{A/4} \left\{1 + \left[\frac{A-4}{6}\right] b_0 p_t^2\right\} \exp(-b_0 p_t^2). \quad (31)$$

It is worth noting that the harmonic oscillator spectral function (29) does not satisfy the energy sum rule (22). So, from (20), (21) and (29) for C^{12} target nucleus one gets:

$$< T >_{MF} = \left(\frac{5A-8}{4A}\right) \frac{1}{m_N b_0} = 16.8\ MeV,$$
$$< E >_{MF} = \frac{4}{A}|\epsilon_{1s}| + \left(\frac{A-4}{A}\right)|\epsilon_{1p}| = 22\ MeV. \quad (32)$$

If the calculated values of $< T >_{MF}$ and $< E >_{MF}$ are placed in the Koltun sum rule (22), the value of $\epsilon_A = -7.0\ MeV$ for C^{12} nucleus [43] is not obtained.

Let us focus now on the correlated part $P_1(\mathbf{p}_t, E)$ of the nucleon spectral function. Results of the many–body calculations with realistic models of the NN interaction in few–body systems, complex nuclei and nuclear matter [16, 17, 19–23] as well as experimental data for nucleon momentum distribution $n(\mathbf{p}_t) = \int P(\mathbf{p}_t, E) dE$ obtained by the y–scaling analysis [18] show that:

i) the momentum distribution $n(\mathbf{p}_t)$ for $p_t > 2 fm^{-1}$ is a several orders of magnitude larger than the predictions from mean–field calculations and, moreover, the high momentum behaviour of $n(\mathbf{p}_t)$ (at $p_t \geq 2 fm^{-1}$) is similar for nuclei with mass number $A \geq 2$;

ii) the behaviour of the nucleon spectral function at high values of p_t and E is almost entirely governed by $P_1(\mathbf{p}_t, E)$ as well as there is a strong coupling between the high momentum components and the high values of the removal energy ($E \sim p_t^2/2m_N$) of a nucleon embedded in the nuclear medium.

Starting from such observation and analyzing the perturbative expansion of the NN interaction and the momentum distribution for potentials decreasing at large values of p_t as powers of p_t, Frankfurt and Strikman have argued [45] that the structure of the nucleon spectral function at high values of nucleon momentum and removal energy should be generated mainly by the ground–state two–nucleon configurations with large relative ($\geq 1.5\ fm^{-1}$), but low ($< 1.5\ fm^{-1}$) center–of–mass momenta. Basing on this assumption, the convolution model for the correlated part $P_1(\mathbf{p}_t, E)$ of the nucleon spectral function in the case of any value of the mass number A has been proposed [19, 21] according to which function $P_1(\mathbf{p}_t, E)$ is expressed as a convolution integral of the momentum distributions describing the relative and center–of–mass motions of a correlated NN pair embedded in the nuclear medium. It was shown [19, 21] that this model satisfactorily reproduces the existing spectral functions of He^3, He^4 and nuclear matter obtained by means of many–body calculations with realistic models of the NN interaction. An inspection of the convolution formula (53) from [21] for the spectral function $P_1(\mathbf{p}_t, E)$ leads to the following simple analytical expression for the $P_1(\mathbf{p}_t, E)$ proposed in [17] (formula (7)):

$$P_1(\mathbf{p}_t, E) = a_1 n_1(\mathbf{p}_t) \times \exp\left\{-3[(A-2)/(A-1)]m_N \times \left[\sqrt{E - E_{thr}} - \sqrt{E_1(p_t) - E_{thr}}\right]^2 / < p_{cm}^2 >\right\}, \quad (33)$$

where

$$a_1 = \frac{3[(A-2)/(A-1)]m_N}{\left\{e^{-\alpha_0^2} + \alpha_0 \sqrt{\pi}\,[1 + erf(\alpha_0)]\right\} < p_{cm}^2 >}, \quad (34)$$

$$\alpha_0 = \frac{p_t}{(< p_{cm}^2 >)^{1/2}} \sqrt{\frac{3}{2}\left(\frac{A-2}{A-1}\right)^2 \left[1 - \left(\frac{A-1}{A-2}\right)\gamma\right]}, \quad (35)$$

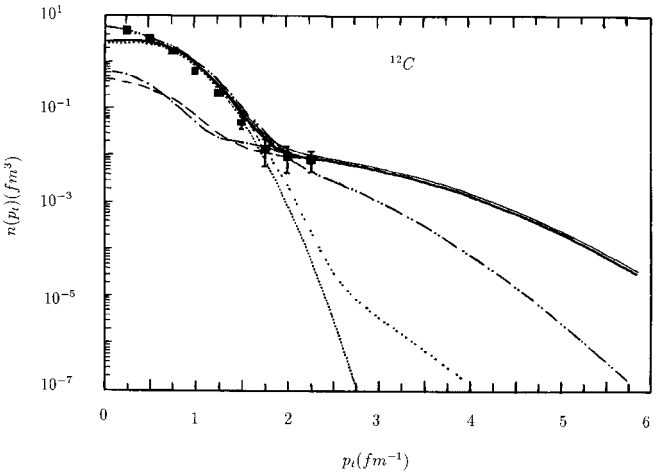

Fig. 2. Momentum distribution for C^{12}. The notations: see text. The normalization of momentum distributions (denoted by $n(p_t)$) which correspond to the *light* and *heavy solid lines*, *dashed line with two dots* and *two dots line* is $\int_0^\infty n(p_t)p_t^2 dp_t = 1$

$$erf(x) = \frac{2}{\sqrt{\pi}} \int_0^x e^{-t^2} dt,$$

$$E_1(p_t) = E_{thr} + \left(\frac{A-2}{A-1}\right) \frac{p_t^2}{2m_N} \left[1 - \left(\frac{A-1}{A-2}\right)\gamma\right], \quad (36)$$

$$\gamma = \frac{< p_{cm}^2 >}{< p_{rel}^2 >}.$$

Here, a_1 is a proper normalization constant (such that $\int_{E_{thr}}^\infty P_1(\mathbf{p}_t, E)dE = n_1(\mathbf{p}_t)$); $E_{thr} = M_{A-2} + 2m_N - M_A$ is the two–particle break–up threshold (in the case of C^{12} target nucleus E_{thr} is equal to 25 MeV [24]); $< p_{cm}^2 >$ and $< p_{rel}^2 >$ are the mean–square momenta associated to the low and high momentum parts of the momentum distribution describing the center–of–mass motion of a correlated NN pair and the momentum distribution describing the relative motion of this pair, respectively. In our calculations of the K^+ production cross sections on C^{12} target nuclei we have used the values $< p_{cm}^2 >= 1.5 fm^{-2}$ and $< p_{rel}^2 >= 7.5 fm^{-2}$ [19, 21]. The many–body momentum distributions $n_1(\mathbf{p}_t)$ and $n_0(\mathbf{p}_t)$ for C^{12} have been presented in [16, 17] (see also Fig. 2, dashed and dotted lines, respectively). Taking into account the normalization of $n_1(\mathbf{p}_t)$ given by (27), it can be parametrized as follows:

$$n_1(\mathbf{p}_t) = \frac{S_1}{(2\pi)^{3/2}(1+\alpha_1)} \quad (37)$$
$$\times \left[\frac{1}{\sigma_1^3} \exp\left(-p_t^2/2\sigma_1^2\right) + \frac{\alpha_1}{\sigma_2^3} \exp\left(-p_t^2/2\sigma_2^2\right)\right],$$

where $\sigma_1^2 = 0.162 fm^{-2}$, $\sigma_2^2 = 2.50 fm^{-2}$ and $\alpha_1 = 2.78$ (dot–dashed line in Figure 2). In this Figure our total nucleon momentum distribution $n(\mathbf{p}_t) = n_0(\mathbf{p}_t) + n_1(\mathbf{p}_t)$ in C^{12} (light solid line) calculated by (31), (37) is compared as well with that obtained using many–body calculations with the Reid V6 interaction [16, 43] (heavy solid line) as well as with the existing experimental data (squares) taken from [18]. It is seen that our total nucleon momentum distribution fits well the many–body one[4] as well as the experimental data. It can also be seen that at $p_t \geq 2fm^{-1}$ the full momentum distribution is entirely exhausted by $n_1(\mathbf{p}_t)$ and at $p_t < 2fm^{-1}$ it is almost totally determined by $n_0(\mathbf{p}_t)$. In Fig. 2 we also show the nucleon momentum distribution extracted in [2, 12] from quasielastic electron scattering and high–energy proton backward scattering (dashed line with two dots) as well as the one inferred in [46] from the "old generation" of $(e, e'p)$ and (γ, p) experiments [13] (two dots line), which are given, respectively, by the formula (37) with $S_1 = 1.0$, $\sigma_1 = 100$ MeV/c, $\sigma_2 = 230$ MeV/c, $\alpha_1 = 0.06$ and by:

$$n(\mathbf{p}_t) = \frac{1}{A/4}\left\{n_{1/2}(\mathbf{p}_t) + \left[\frac{A-4}{4}\right] n_{3/2}(\mathbf{p}_t)\right\}, \quad (38)$$

where

$$n_{1/2}(\mathbf{p}_t) = (\pi\nu)^{-3/2} \exp\left(-p_t^2/\nu\right), \quad (39)$$
$$n_{3/2}(\mathbf{p}_t) = C_1 n_{HO}(\mathbf{p}_t) + C_2 n_{exp}(\mathbf{p}_t), \quad (40)$$
$$n_{HO}(\mathbf{p}_t) = \frac{2}{3}(\pi\nu)^{-3/2}(p_t^2/\nu) \exp\left(-p_t^2/\nu\right), \quad (41)$$
$$n_{exp}(\mathbf{p}_t) = \left[\frac{1}{24\pi(p_t^0)^3}\right](p_t/p_t^0) \exp\left(-p_t/p_t^0\right) \quad (42)$$

and $\sqrt{\nu} = 127.0$ MeV/c, $p_t^0 = 55.0$ MeV/c, $C_1 = 0.997$, $C_2 = 0.003$. These nucleon momentum distributions are widely used (see, e.g., [2, 4, 38]) in calculations of the subthreshold particles production in proton–nucleus interactions. One can see that the many–body momentum distribution is substantially larger than the distributions mentioned above at $p_t > 2fm^{-1}$. It should also be pointed out that the full nucleon spectral function presented by (18), (28) and (33), in particular, gives for the mean kinetic $< T >$ and removal $< E >$ energies the values of 37 and 46 MeV, respectively, which agree well with those ($< T >= 37$ MeV and $< E >= 49$ MeV) obtained from many–body calculations [16].

Before closing this subsection, let us consider two approximated forms for the spectral function $P_1(\mathbf{p}_t, E)$, which have been employed earlier in the calculations of inclusive processes at high energy and momentum transfer [16, 17]. It is interesting to use these forms also in the calculations of subthreshold kaon production in pA interactions. Equation (33) shows that if $< p_{cm}^2 > \to 0$, the spectral function $P_1(\mathbf{p}_t, E)$ will have the following δ–function form [19, 21]:

$$P_1(\mathbf{p}_t, E) = n_1(\mathbf{p}_t)\delta\left[E - E_1(p_t)\right] \quad (43)$$

with

$$E_1(p_t) = E_{thr} + \left(\frac{A-2}{A-1}\right)\frac{p_t^2}{2m_N}. \quad (44)$$

[4] It should be mentioned that our uncorrelated momentum distribution $n_0(\mathbf{p}_t)$ given by (31) practically coincides with the many–body one. Therefore, we did not show it in Fig. 2

The model given by (43) and (44) is called the two–nucleon correlation (2NC) model [19, 21]. The other model for function $P_1(\mathbf{p}_t, E)$ is also δ–function model in which only the mean value of the energy associated with the excited configurations is taken into account, namely [16, 17]:

$$P_1(\mathbf{p}_t, E) = n_1(\mathbf{p}_t)\delta\left(E - \bar{E}_1\right), \qquad (45)$$

where $\bar{E}_1$ can easily be obtained from the definition of the mean removal energy $< E >$ and it is equal to 157 MeV in the case of C^{12} target nucleus. The expressions (28), (33), (43) and (45) for the respective spectral functions were used in our calculations of K^+ production in pC collisions.

1.3 Direct K^+ production processes: results and discussion

The comparison of the results of our calculations by (3)–(13), (17), (18), (28)–(30), (33)–(37) and (43)–(45) with the experimental data [8] and calculations in the framework of the first chance collision model [8] with the nucleon spectral function taken from [20, 27] for the double differential cross sections for the production of K^+ mesons at an angle of 40^0 from primary channels (1), (2) in the interaction of protons with energies of 1.2, 1.5 and 2.5 GeV with C^{12} nuclei is given in Fig. 3. One can see that:

1) our results coming from the use of the total nucleon spectral function $P(\mathbf{p}_t, E)$ in simple form (18), (28) and (33) are in reasonable agreement with the 2.5 GeV data as well as with the calculations within the first chance collision model [8] with elaborate spectral function [20, 27], based on the application of the local density approximation to the correlated part $P_1(\mathbf{p}_t, E)$;
2) the high momentum tail of the kaon spectrum at 2.5 GeV beam energy is entirely governed by $P_1(\mathbf{p}_t, E)$ and what is more, the δ–function models (43) and (45) for the spectral function $P_1(\mathbf{p}_t, E)$ yield in the high momentum part of the kaon spectrum essentially different results with respect to the model (33) in which the energy dependence of $P_1(\mathbf{p}_t, E)$ is taken into account;
3) our model, along with the first chance collision model [8], fails completely to reproduce the experimental data at 1.2 and 1.5 GeV incident energies;
4) our results at these initial energies are about a factor of 3–5 below those obtained within the first chance collision model [8], this difference may be due to the different elementary kaon production cross sections and different spectral functions employed in the work presented here and in approach [8];
5) the main contribution to the K^+ production at 1.2 GeV beam energy comes from the use in the calculations only of the correlated part $P_1(\mathbf{p}_t, E)$ of the nucleon spectral function, the cross sections calculated with the spectral function (33) are sufficiently close to those obtained with the spectral function in the δ–function form (45)[5].

[5] The 2NC model (43) does not contribute to the K^+ production at all at this beam energy

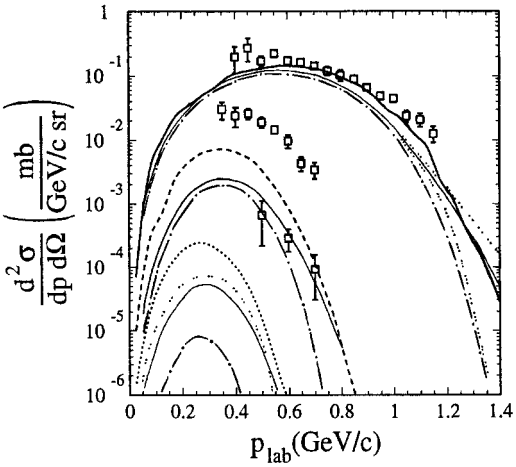

Fig. 3. Double differential cross sections for the production of K^+ mesons at an angle of 40^0 in the interaction of protons with energies of 1.2, 1.5 and 2.5 GeV with C^{12} nuclei as a functions of kaon momentum. The *data points* [8] correspond from the top to the bottom 2.5, 1.5 and 1.2 GeV beam energy, respectively. The *heavy solid*, *dashed* and *dotted lines* are calculations within the first chance collision model [8] with the nucleon spectral function taken from [20, 27] at 2.5, 1.5 and 1.2 GeV beam energies, respectively. The *light solid* and *dot–dashed lines* represent our calculations by (3) for primary production processes (1), (2) with the use of total nucleon spectral function and its uncorrelated part, respectively, and correspond from the top to the bottom 2.5, 1.5 and 1.2 GeV incident energy. The *three dots* and *two dots lines* denote the same as *light solid line*, but it is supposed that the correlated part of the nucleon spectral function given by (33) is replaced by its δ–function forms (43) and (45), respectively

Thus, the presented above results, both our and those from [8], obtained using different nucleon spectral functions show that the direct K^+ production processes (1), (2) play a minor role in subthreshold kaon production in pA collisions and additional kaon production mechanisms are needed to explain the data under consideration.

Let us consider now the two–step K^+ production mechanism.

2 Two–Step K^+ production processes

2.1 Kaon production cross section

Kinematical considerations show that in the bombarding energy range of our interest ($\leq$ 2.5 GeV) the following two–step production processes may not only contribute to the K^+ production in pA interactions but even dominate [1, 3–5, 8, 9] at subthreshold energies ($\leq$ 1.5 GeV). An incident proton can produce in the first inelastic collision with an intranuclear nucleon also a pion through the elementary reactions:

$$p + N_1 \rightarrow N + N + \pi, \qquad (46)$$

$$p + N_1 \rightarrow N + N + 2\pi. \qquad (47)$$

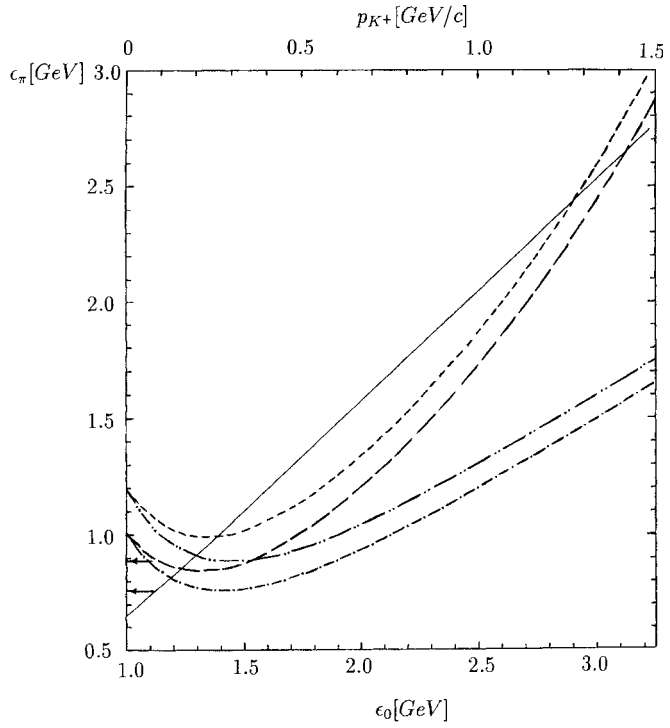

Fig. 4. Maximum kinetic energy of a pion produced by a proton on a target nucleon at rest as a function of the kinetic energy ϵ_0 of a proton–*solid line*. Kinetic energy of a pion that is needed for the production of a kaon on a target nucleon at rest in reactions (48), (49) at the angles of 0^0–*dashed lines with one* and *two dots*, respectively, and 40^0–*long*– and *short–dashed lines*, respectively, as a function of the kaon momentum p_{K^+}. The *arrows* show the free thresholds for these reactions

We remind that the free threshold energies for these reactions respectively are 0.29 and 0.60 GeV. Then the intermediate pion, which is assumed to be on–shell, produces the kaon on a nucleon of the target nucleus via the elementary subprocesses with the lowest free production thresholds (respectively, 0.76 and 0.89 GeV):

$$\pi + N_2 \to K^+ + \Lambda, \tag{48}$$

$$\pi + N_2 \to K^+ + \Sigma, \tag{49}$$

provided that these subprocesses are energetically possible. So, in Fig. 4 we show the maximum kinetic energy ϵ_π^{max} of a pion produced by a proton on a target nucleon at rest as a function of the kinetic energy ϵ_0 (lower axis) of a proton as well as the kinetic energy ϵ_π of a pion which is needed for the production of a kaon on a target nucleon at rest at the angles of 0^0 and 40^0 in the laboratory frame in reactions (48), (49) as a function of the momentum p_{K^+} (upper axis) of a kaon. The quantities ϵ_π^{max} and ϵ_π were calculated according to the following expressions:

$$\epsilon_\pi^{max} = \sqrt{\left(p_\pi^{max}\right)^2 + m_\pi^2} - m_\pi,$$
$$p_\pi^{max} = \left[\beta p_0 + (E_0 + m_N)\sqrt{\beta^2 - 4m_\pi^2 s}\right]/(2s), \tag{50}$$

$$\beta = s + m_\pi^2 - 4m_N^2,$$

$$s = (E_0 + m_N)^2 - p_0^2 = 2m_N(\epsilon_0 + 2m_N);$$

$$\epsilon_\pi = \frac{\beta_1(m_N - E_{K^+}) - p_{K^+}|\cos\vartheta_{K^+}|\sqrt{\beta_1^2 - 4m_\pi^2\tilde{s}}}{2\tilde{s}} - m_\pi, \tag{51}$$

$$\tilde{s} = (m_N - E_{K^+})^2 - p_{K^+}^2\cos^2\vartheta_{K^+},$$

$$\beta_1 = m_Y^2 - m_N^2 - m_K^2 - m_\pi^2 + 2m_N E_{K^+}.$$

Here, m_π is the rest mass of a pion, $\cos\vartheta_{K^+} = \mathbf{p}_0\mathbf{p}_{K^+}/p_0 p_{K^+}$. It is seen, for instance, that at $\epsilon_0 = 1.2\ GeV$, $\vartheta_{K^+} = 40^0$, $p_{K^+} = 0.5\ GeV/c$ the K^+ production processes (48), (49) can take place only if the target nucleon carries a momentum inside the nucleus and at $\epsilon_0 = 1.5\ GeV$ there is a region of pion's energy where the K^+ production process (48) for the same values of ϑ_{K^+} and p_{K^+} as above occurs even if the intranuclear nucleon is at rest.

In order to calculate the K^+ production cross section for pA reactions from the secondary pion induced reaction channels (48) and (49), it is necessary to fold the inclusive differential cross section for pion production in the reactions (46), (47) (denoted by $d\sigma_{pN\to\pi X}/d\mathbf{p}_\pi$), calculated for given internal momentum $\mathbf{p}_t$ and removal energy E of the target nucleon N_1, with the momentum–energy–averaged inclusive invariant differential cross section for K^+ production in these channels (denoted by $\int\int P(\mathbf{p'}_t, E')d\mathbf{p'}_t dE'[E_{K^+}d\sigma_{\pi N\to K^+X}/d\mathbf{p}_{K^+}]$) and with the effective number of N_1N_2 pairs per unit of area (denoted via $I_V[A, \sigma_{pN}^{in}(p_0), \sigma_{\pi N}^{tot}(p_\pi), \vartheta_\pi]$), involved in the two–step kaon production processes under consideration, and then to average this result over $\mathbf{p}_t$ and E, i.e. (see, also, [38]):

$$E_{K^+}\frac{d\sigma_{pA\to K^+X}^{(sec)}(\mathbf{p}_0)}{d\mathbf{p}_{K^+}} = \sum_{i,j=0,1} E_{K^+}\frac{d\sigma_{ij}^{(sec)}(\mathbf{p}_0)}{d\mathbf{p}_{K^+}}, \tag{52}$$

where

$$E_{K^+}\frac{d\sigma_{ij}^{(sec)}(\mathbf{p}_0)}{d\mathbf{p}_{K^+}} = \sum_{\pi=\pi^+,\pi^0,\pi^-}\int\int P_i(\mathbf{p}_t, E)d\mathbf{p}_t dE \tag{53}$$
$$\times \int_{p_\pi^{abs}}^{p_\pi^{max}(\mathbf{p}_t,E)} p_\pi^2 dp_\pi \int_{4\pi} d\mathbf{\Omega}_\pi I_V[A, \sigma_{pN}^{in}(p_0), \sigma_{\pi N}^{tot}(p_\pi), \vartheta_\pi]$$
$$\times \frac{d\sigma_{pN\to\pi X}(\sqrt{s}, \mathbf{p}_\pi)}{d\mathbf{p}_\pi}$$
$$\times \int\int P_j(\mathbf{p'}_t, E')d\mathbf{p'}_t dE'\left[E_{K^+}\frac{d\sigma_{\pi N\to K^+X}(\sqrt{s_1}, \mathbf{p}_{K^+})}{d\mathbf{p}_{K^+}}\right]$$

and

$$I_V[A,\sigma_{pN}^{in}(p_0),\sigma_{\pi N}^{tot}(p_\pi),\vartheta_\pi] \quad (54)$$
$$= A^2\int\int d\mathbf{r}d\mathbf{r}_1\Theta(x_\parallel)\delta^{(2)}(\mathbf{x}_\perp)\rho(\mathbf{r})\rho(\mathbf{r}_1)$$
$$\times\exp[-\mu(p_0)\int\limits_{-\infty}^{0}\rho(\mathbf{r}_1+x'\boldsymbol{\Omega}_0)dx'$$
$$-\mu(p_\pi)\int\limits_{0}^{x_\parallel}\rho(\mathbf{r}_1+x'\boldsymbol{\Omega}_\pi)dx'],$$

$$\mathbf{r}-\mathbf{r}_1=x_\parallel\boldsymbol{\Omega}_\pi+\mathbf{x}_\perp,\boldsymbol{\Omega}_\pi=\mathbf{p}_\pi/p_\pi,\cos\vartheta_\pi=\boldsymbol{\Omega}_0\boldsymbol{\Omega}_\pi; \quad (55)$$
$$\mu(p_\pi)=(A/2)[\sigma_{\pi p}^{tot}(p_\pi)+\sigma_{\pi n}^{tot}(p_\pi)],$$
$$\Theta(x_\parallel)=(x_\parallel+|x_\parallel|)/2|x_\parallel|;$$

$$\frac{d\sigma_{pN\to\pi X}(\sqrt{s},\mathbf{p}_\pi)}{d\mathbf{p}_\pi}=\frac{Z}{A}\frac{d\sigma_{pp\to\pi X}(\sqrt{s},\mathbf{p}_\pi)}{d\mathbf{p}_\pi} \quad (56)$$
$$+\frac{N}{A}\frac{d\sigma_{pn\to\pi X}(\sqrt{s},\mathbf{p}_\pi)}{d\mathbf{p}_\pi},$$

$$E_{K^+}\frac{d\sigma_{\pi N\to K^+X}(\sqrt{s_1},\mathbf{p}_{K^+})}{d\mathbf{p}_{K^+}} \quad (57)$$
$$=\frac{Z}{A}E_{K^+}\frac{d\sigma_{\pi p\to K^+X}(\sqrt{s_1},\mathbf{p}_{K^+})}{d\mathbf{p}_{K^+}}$$
$$+\frac{N}{A}E_{K^+}\frac{d\sigma_{\pi n\to K^+X}(\sqrt{s_1},\mathbf{p}_{K^+})}{d\mathbf{p}_{K^+}};$$

$$s_1=(E_\pi+E_t^{'})^2-(\mathbf{p}_\pi+\mathbf{p'}_t)^2, \quad (58)$$

$$E_t^{'}=\begin{cases}M_A-E_t & \text{for } i=0,\\ -\sqrt{(-\mathbf{p}_t-\mathbf{p'}_t)^2+(M_A-2m_N+E+E')^2} & j=0,1\\ M_{A-2}-\sqrt{(-\mathbf{p'}_t)^2+(M_{A-2}-m_N+E')^2} & \text{for } i=1,\\ & j=0,1\end{cases}; \quad (59)$$

$$p_\pi^{max}(\mathbf{p}_t,E) \quad (60)$$
$$=\left[\beta|\mathbf{p}_0+\mathbf{p}_t|+(E_0+E_t)\sqrt{\beta^2-4m_\pi^2 s}\right]/(2s).$$

Here, $d\sigma_{pp\to\pi X}/d\mathbf{p}_\pi$ ($d\sigma_{pn\to\pi X}/d\mathbf{p}_\pi$) is the free inclusive differential cross section for pion production in pp (pn) collisions through the elementary reactions (46), (47); $E_{K^+}d\sigma_{\pi p\to K^+X}/d\mathbf{p}_{K^+}$ ($E_{K^+}d\sigma_{\pi n\to K^+X}/d\mathbf{p}_{K^+}$) is the free inclusive invariant differential cross section for K^+ production in πp (πn) collisions via the subprocesses (48), (49); $\sigma_{\pi N}^{tot}(p_\pi)$ is the total cross section of the free πN interaction; $\mathbf{p}_\pi$ and E_π are the momentum and total energy of a pion; p_π^{abs} is the absolute threshold momentum for kaon production on the residual nucleus by an intermediate pion[6]. The quantities $\mu(p_0)$, s and β are defined above by the (5), (7) and (50), respectively.

[6] Calculations show that $p_\pi^{abs}\approx 0.69$ GeV/c and $p_\pi^{abs}\approx 0.77$ GeV/c for the production of $K^+\Lambda$ and $K^+\Sigma$ systems, respectively

In our method the differential cross sections $d\sigma_{pp\to\pi X}/d\mathbf{p}_\pi$ and $d\sigma_{pn\to\pi X}/d\mathbf{p}_\pi$ for pion production in pp and pn collisions have been described by the three– and four–body phase space calculations normalized to the respective total cross sections. According to (9) and [29], one has:

$$E_{\pi^+}\frac{d\sigma_{pp\to\pi^+X}(\sqrt{s},\mathbf{p}_{\pi^+})}{d\mathbf{p}_{\pi^+}}=\sigma_{pp\to pn\pi^+}(\sqrt{s})f_3(s,\mathbf{p}_{\pi^+})$$
$$+\left[\sigma_{pp\to pp\pi^+\pi^-}(\sqrt{s})+\sigma_{pp\to pn\pi^+\pi^0}(\sqrt{s})\right.$$
$$\left.+2\sigma_{pp\to nn\pi^+\pi^+}(\sqrt{s})\right]\times f_4(s,\mathbf{p}_{\pi^+}), \quad (61)$$

$$E_{\pi^0}\frac{d\sigma_{pp\to\pi^0X}(\sqrt{s},\mathbf{p}_{\pi^0})}{d\mathbf{p}_{\pi^0}}=\sigma_{pp\to pp\pi^0}(\sqrt{s})f_3(s,\mathbf{p}_{\pi^0}) \quad (62)$$
$$+\left[\sigma_{pp\to pn\pi^+\pi^0}(\sqrt{s})+2\sigma_{pp\to pp\pi^0\pi^0}(\sqrt{s})\right]f_4(s,\mathbf{p}_{\pi^0}),$$

$$E_{\pi^-}\frac{d\sigma_{pp\to\pi^-X}(\sqrt{s},\mathbf{p}_{\pi^-})}{d\mathbf{p}_{\pi^-}}=\sigma_{pp\to pp\pi^+\pi^-}(\sqrt{s}) \quad (63)$$
$$\times f_4(s,\mathbf{p}_{\pi^-});$$

$$E_{\pi^+}\frac{d\sigma_{pn\to\pi^+X}(\sqrt{s},\mathbf{p}_{\pi^+})}{d\mathbf{p}_{\pi^+}}=\sigma_{pn\to nn\pi^+}(\sqrt{s})f_3(s,\mathbf{p}_{\pi^+}) \quad (64)$$
$$+\left[\sigma_{pn\to pn\pi^+\pi^-}(\sqrt{s})+\sigma_{pn\to nn\pi^+\pi^0}(\sqrt{s})\right]f_4(s,\mathbf{p}_{\pi^+}),$$

$$E_{\pi^0}\frac{d\sigma_{pn\to\pi^0X}(\sqrt{s},\mathbf{p}_{\pi^0})}{d\mathbf{p}_{\pi^0}}=\sigma_{pn\to pn\pi^0}(\sqrt{s})f_3(s,\mathbf{p}_{\pi^0}) \quad (65)$$
$$+\left[\sigma_{pn\to nn\pi^+\pi^0}(\sqrt{s})+\sigma_{pn\to pp\pi^-\pi^0}(\sqrt{s})\right.$$
$$\left.+2\sigma_{pn\to pn\pi^0\pi^0}(\sqrt{s})\right]\times f_4(s,\mathbf{p}_{\pi^0}),$$

$$E_{\pi^-}\frac{d\sigma_{pn\to\pi^-X}(\sqrt{s},\mathbf{p}_{\pi^-})}{d\mathbf{p}_{\pi^-}}=E_{\pi^+}\frac{d\sigma_{pn\to\pi^+X}(\sqrt{s},\mathbf{p}_{\pi^+})}{d\mathbf{p}_{\pi^+}}; \quad (66)$$

where

$$f_3(s,\mathbf{p}_\pi)=\frac{\pi}{4I_3(s,m_\pi,m_N,m_N)}\frac{\lambda(s_{NN},m_N^2,m_N^2)}{s_{NN}}, \quad (67)$$

$$s_{NN}=s+m_\pi^2-2(E_0+E_t)E_\pi+2(\mathbf{p}_0+\mathbf{p}_t)\mathbf{p}_\pi \quad (68)$$

and

$$f_4(s,\mathbf{p}_\pi) \quad (69)$$
$$=I_3(s_{NN\pi},m_\pi,m_N,m_N)/\left[2I_4(s,m_\pi,m_\pi,m_N,m_N)\right],$$

$$I_4(s,m_\pi,m_\pi,m_N,m_N) \quad (70)$$
$$=\frac{\pi}{2}\int\limits_{4m_N^2}^{(\sqrt{s}-2m_\pi)^2}\frac{\lambda(s_{NN},m_N^2,m_N^2)}{s_{NN}}\times$$
$$\times I_3(s,m_\pi,\sqrt{s_{NN}},m_\pi)ds_{NN},$$

$$s_{NN\pi}=s+m_\pi^2-2(E_0+E_t)E_\pi+2(\mathbf{p}_0+\mathbf{p}_t)\mathbf{p}_\pi. \quad (71)$$

For the total cross sections $\sigma_{pN\to NN\pi}$ and $\sigma_{pN\to NN2\pi}$ entering into the Eqs. (61)–(65) we used the parametrization suggested in [47]:

$$\sigma_k = \begin{cases} 0 & \text{for } \epsilon_0 \le \epsilon_{thr}^{(k)} \\ |F^k(x)|^2 & \text{for } \epsilon_0 > \epsilon_{thr}^{(k)}, \end{cases} \tag{72}$$

where

$$F^k(x) = \sum_{n=0}^{\infty} a_n^k L_n^2(x), \quad x = \ln(\epsilon_0/\epsilon_{thr}^{(k)}). \tag{73}$$

Here, the expansion functions $L_n^2(x)$ are Laguerre polynomials and $\epsilon_{thr}^{(k)}$ is the threshold energy for the considered reaction k. The parameters a_n^k in (73) were adjusted to the available experimental data and are given in [47][7].

Taking into account the two–body kinematics of the elementary processes (48), (49), we can readily get the following expression for the Lorentz invariant inclusive cross sections for these processes:

$$E_{K^+}\frac{d\sigma_{\pi N\to K^+Y}(\sqrt{s_1},\mathbf{p}_{K^+})}{d\mathbf{p}_{K^+}} = \frac{\pi}{I_2(s_1,m_Y,m_K)}\frac{d\sigma_{\pi N\to K^+Y}(s_1)}{d\overset{*}{\mathbf{\Omega}}} \times\frac{1}{(\omega+E_t^{'})}\delta\left[\omega+E_t^{'}-\sqrt{m_Y^2+(\mathbf{Q}+\mathbf{p'}_t)^2}\right], \tag{74}$$

$$I_2(s_1,m_Y,m_K) = \frac{\pi}{2}\frac{\lambda(s_1,m_Y^2,m_K^2)}{s_1}, \tag{75}$$

$$\omega = E_\pi - E_{K^+},\ \mathbf{Q} = \mathbf{p}_\pi - \mathbf{p}_{K^+},\ E_\pi = \sqrt{p_\pi^2+m_\pi^2}. \tag{76}$$

Here, $d\sigma_{\pi N\to K^+Y}(s_1)/d\overset{*}{\mathbf{\Omega}}$ are the K^+ differential cross sections in the πN center–of–mass system. According to Cugnon et al. [48], we choose the K^+ angular distributions in the following forms:

$$\frac{d\sigma_{\pi^+n\to K^+\Lambda}(s_1)}{d\overset{*}{\mathbf{\Omega}}} = [1+A_1(\sqrt{s_1})\cos\overset{*}{\vartheta}_{K^+}] \times\frac{\sigma_{\pi^+n\to K^+\Lambda}(\sqrt{s_1})}{4\pi}, \tag{77}$$

$$\frac{d\sigma_{\pi^0p\to K^+\Lambda}(s_1)}{d\overset{*}{\mathbf{\Omega}}} = \frac{1}{2}\frac{d\sigma_{\pi^+n\to K^+\Lambda}(s_1)}{d\overset{*}{\mathbf{\Omega}}}, \tag{78}$$

$$\frac{d\sigma_{\pi N\to K^+\Sigma}(s_1)}{d\overset{*}{\mathbf{\Omega}}} = [1+|\cos\overset{*}{\vartheta}_{K^+}|]\frac{\sigma_{\pi N\to K^+\Sigma}(\sqrt{s_1})}{6\pi}. \tag{79}$$

[7] We used in calculations the following correct values of these parameters obtained by us for the $pp\to pn\pi^+$, $pp\to pn\pi^+\pi^0$ and $pn\to pn\pi^+\pi^-$ reactions: $a_n^{pp\to pn\pi^+}$ = {−2.3535, 3.9869, −6.8338, −4.3856, 6.2068, 7.3596, −4.0343, −7.2470, −2.3034, 11.9020, −5.3132}, $a_n^{pp\to pn\pi^+\pi^0}$ = {11.3270, −6.9858, −2.9822, 2.8256}, $a_n^{pn\to pn\pi^+\pi^-}$ = {−8.5595, 9.4735, −8.3943, 3.1530}

The parameter A_1 and the total cross section $\sigma_{\pi^+n\to K^+\Lambda}$ of reaction $\pi^+n\to K^+\Lambda$ can be parametrized by [48]:

$$A_1(\sqrt{s_1}) = \begin{cases} 5.26\left(\frac{\sqrt{s_1}-\sqrt{s_0}}{\text{GeV}}\right) & \text{for } \sqrt{s_0}<\sqrt{s_1}\le 1.8 \text{ GeV} \\ 1 & \text{for } \sqrt{s_1}>1.8 \text{ GeV}, \end{cases} \tag{80}$$

$$\sigma_{\pi^+n\to K^+\Lambda}(\sqrt{s_1}) = \begin{cases} 10.0\left(\frac{\sqrt{s_1}-\sqrt{s_0}}{\text{GeV}}\right)\ [\text{mb}] & \text{for } \sqrt{s_0}<\sqrt{s_1}\le 1.7 \text{ GeV} \\ 0.09\left(\frac{\text{GeV}}{\sqrt{s_1}-1.6\text{GeV}}\right)\ [\text{mb}] & \text{for } \sqrt{s_1}>1.7 \text{ GeV}, \end{cases} \tag{81}$$

where $\sqrt{s_0} = m_K + m_\Lambda = 1.61$ GeV is the threshold energy. For the total cross sections $\sigma_{\pi N\to K^+\Sigma}(\sqrt{s_1})$ we have used the following parametrization suggested in [49] on a basis of the resonance–model calculations:

$$\sigma_{\pi N\to K^+\Sigma}(\sqrt{s_1}) = \sum_{n=1}^{2}\frac{d_n(\sqrt{s_1}-\sqrt{\tilde{s}_0})^{f_n}}{(\sqrt{s_1}-c_n)^2+b_n}, \tag{82}$$

where $\sqrt{\tilde{s}_0} = m_K + m_\Sigma = 1.688$ GeV is the threshold energy and the constants d_n, b_n, c_n and f_n are given in Table 2. Within the representation (74), the inclusive invariant differential cross sections $E_{K^+}d\sigma_{\pi p\to K^+X}/d\mathbf{p}_{K^+}$ and $E_{K^+}d\sigma_{\pi n\to K^+X}/d\mathbf{p}_{K^+}$ for kaon production in πp and πn interactions appearing in the Eq. (57) can be written in the following forms:

$$E_{K^+}\frac{d\sigma_{\pi^+p\to K^+X}(\sqrt{s_1},\mathbf{p}_{K^+})}{d\mathbf{p}_{K^+}} = E_{K^+}\frac{d\sigma_{\pi^+p\to K^+\Sigma^+}(\sqrt{s_1},\mathbf{p}_{K^+})}{d\mathbf{p}_{K^+}},$$
$$E_{K^+}\frac{d\sigma_{\pi^+n\to K^+X}(\sqrt{s_1},\mathbf{p}_{K^+})}{d\mathbf{p}_{K^+}} = E_{K^+}\frac{d\sigma_{\pi^+n\to K^+\Lambda}(\sqrt{s_1},\mathbf{p}_{K^+})}{d\mathbf{p}_{K^+}} + E_{K^+}\frac{d\sigma_{\pi^+n\to K^+\Sigma^0}(\sqrt{s_1},\mathbf{p}_{K^+})}{d\mathbf{p}_{K^+}}; \tag{83}$$

$$E_{K^+}\frac{d\sigma_{\pi^0p\to K^+X}(\sqrt{s_1},\mathbf{p}_{K^+})}{d\mathbf{p}_{K^+}} = E_{K^+}\frac{d\sigma_{\pi^0p\to K^+\Lambda}(\sqrt{s_1},\mathbf{p}_{K^+})}{d\mathbf{p}_{K^+}} + E_{K^+}\frac{d\sigma_{\pi^0p\to K^+\Sigma^0}(\sqrt{s_1},\mathbf{p}_{K^+})}{d\mathbf{p}_{K^+}},$$
$$E_{K^+}\frac{d\sigma_{\pi^0n\to K^+X}(\sqrt{s_1},\mathbf{p}_{K^+})}{d\mathbf{p}_{K^+}} = E_{K^+}\frac{d\sigma_{\pi^0n\to K^+\Sigma^-}(\sqrt{s_1},\mathbf{p}_{K^+})}{d\mathbf{p}_{K^+}};$$
$$E_{K^+}\frac{d\sigma_{\pi^-p\to K^+X}(\sqrt{s_1},\mathbf{p}_{K^+})}{d\mathbf{p}_{K^+}} = E_{K^+}\frac{d\sigma_{\pi^-p\to K^+\Sigma^-}(\sqrt{s_1},\mathbf{p}_{K^+})}{d\mathbf{p}_{K^+}}, \tag{84}$$

Table 2. Parameters in the approximation of the partial cross sections for the production of K^+ mesons in πN–collisions

Reaction	n	d_n,mb	f_n	c_n,GeV	b_n,GeV^2
$\pi^+ + p \to K^+ + \Sigma^+$	1	0.03591	0.9541	1.890	0.01548
$\pi^+ + p \to K^+ + \Sigma^+$	2	0.1594	0.01056	3.000	0.9412
$\pi^+ + n \to K^+ + \Sigma^0$	1	0.05014	1.2878	1.730	0.006455
$\pi^+ + n \to K^+ + \Sigma^0$	2	—	—	—	—
$\pi^0 + n \to K^+ + \Sigma^-$	1	0.05014	1.2878	1.730	0.006455
$\pi^0 + n \to K^+ + \Sigma^-$	2	—	—	—	—
$\pi^0 + p \to K^+ + \Sigma^0$	1	0.003978	0.5848	1.740	0.006670
$\pi^0 + p \to K^+ + \Sigma^0$	2	0.04709	2.1650	1.905	0.006358
$\pi^- + p \to K^+ + \Sigma^-$	1	0.009803	0.6021	1.742	0.006583
$\pi^- + p \to K^+ + \Sigma^-$	2	0.006521	1.4728	1.940	0.006248

$$E_{K^+}\frac{d\sigma_{\pi^- n\to K^+X}(\sqrt{s_1},\mathbf{p}_{K^+})}{d\mathbf{p}_{K^+}}=0. \quad (85)$$

Let us now simplify the expression (53) for the invariant differential cross section for K^+ production in pA interactions from the two–step processes. Taking into account that the main contribution to the K^+ production comes from fast pions moving in the beam direction and that the πN total cross section $\sigma^{tot}_{\pi N}$ in the energy region of interest is approximately constant with a magnitude of $<\sigma^{tot}_{\pi N}>\approx 35$ mb [50], we have:

$$\begin{aligned}E_{K^+}\frac{d\sigma^{(sec)}_{ij}(\mathbf{p}_0)}{d\mathbf{p}_{K^+}} &= I_V[A,\sigma^{in}_{pN}(p_0),<\sigma^{tot}_{\pi N}>,0^0] \quad (86)\\ &\times\sum_{\pi=\pi^+,\pi^0,\pi^-}\int\int P_i(\mathbf{p}_t,E)d\mathbf{p}_t dE\\ &\times\int\limits_{p^{abs}_\pi}^{p^{max}_\pi(\mathbf{p}_t,E)} dp_\pi\frac{d\sigma_{pN\to\pi X}(\sqrt{s},p_\pi)}{dp_\pi}\\ &\times\iint P_j(\mathbf{p'}_t,E')d\mathbf{p'}_t dE'\\ &\times\left[E_{K^+}\frac{d\sigma_{\pi N\to K^+X}(\sqrt{s_1},\mathbf{p}_{K^+})}{d\mathbf{p}_{K^+}}\right],\end{aligned}$$

where

$$\begin{aligned}&d\sigma_{pN\to\pi X}(\sqrt{s},p_\pi)/dp_\pi \quad (87)\\ &=\int\limits_{4\pi} d\boldsymbol{\Omega}_\pi d^2\sigma_{pN\to\pi X}(\sqrt{s},\mathbf{p}_\pi)/dp_\pi d\boldsymbol{\Omega}_\pi\end{aligned}$$

and according to (58)

$$s_1=(E_\pi+E'_t)^2-(p_\pi\boldsymbol{\Omega}_0+\mathbf{p'}_t)^2. \quad (88)$$

Now let us perform an averaging of the $\pi N\to K^+X$ inclusive invariant differential cross sections (57), (83)–(85) over the Fermi motion of the nucleons in the nucleus using the properties of the Dirac δ–function. Taking into consideration that the struck target nucleon total energy E'_t given by (59) can be approximately represented in the form[8]

$$E'_t\approx<E_t'>=m_N-E'-C_{rec}, \quad (89)$$

in which the quantity C_{rec} takes properly into account the recoil energies of the residual nuclei in the two–step production processes ($C_{rec}\approx 2\ MeV$ for $j=0$ and $C_{rec}\approx 12\ MeV$ for $j=1$ in the case of initial C^{12} target nucleus) as well as choosing the spherical coordinates in $\mathbf{p'}_t$ space with z axis parallel to $\mathbf{Q}$ (see, formulas (74)–(76)) and using the advantage of the spherical symmetry of the spectral function $P_j(\mathbf{p'}_t,E')$ we get the following expression for the cross section (86) after the integration over the angle between $\mathbf{Q}$ and $\mathbf{p'}_t$ and a few other manipulations:

$$\begin{aligned}E_{K^+}\frac{d\sigma^{(sec)}_{ij}(\mathbf{p}_0)}{d\mathbf{p}_{K^+}} &= I_V[A,\sigma^{in}_{pN}(p_0),<\sigma^{tot}_{\pi N}>,0^0] \quad (90)\\ &\times\sum_{\pi=\pi^+,\pi^0,\pi^-}\int\int P_i(\mathbf{p}_t,E)d\mathbf{p}_t dE\\ &\times\int\limits_{p^{abs}_\pi}^{p^{max}_\pi(\mathbf{p}_t,E)} dp_\pi\frac{d\sigma_{pN\to\pi X}(\sqrt{s},p_\pi)}{dp_\pi}\\ &\times\left\langle E_{K^+}\frac{d\sigma_{\pi N\to K^+X}(p_\pi,\mathbf{p}_{K^+})}{d\mathbf{p}_{K^+}}\right\rangle_j,\end{aligned}$$

where

$$\begin{aligned}&\left\langle E_{K^+}\frac{d\sigma_{\pi N\to K^+X}(p_\pi,\mathbf{p}_{K^+})}{d\mathbf{p}_{K^+}}\right\rangle_j = \quad (91)\\ &=\frac{Z}{A}\left\langle E_{K^+}\frac{d\sigma_{\pi p\to K^+X}(p_\pi,\mathbf{p}_{K^+})}{d\mathbf{p}_{K^+}}\right\rangle_j+\\ &+\frac{N}{A}\left\langle E_{K^+}\frac{d\sigma_{\pi n\to K^+X}(p_\pi,\mathbf{p}_{K^+})}{d\mathbf{p}_{K^+}}\right\rangle_j\end{aligned}$$

and

$$\begin{aligned}&\left\langle E_{K^+}\frac{d\sigma_{\pi^+ p\to K^+X}(p_\pi,\mathbf{p}_{K^+})}{d\mathbf{p}_{K^+}}\right\rangle_j=\\ &=\left\langle E_{K^+}\frac{d\sigma_{\pi^+ p\to K^+\Sigma^+}(p_\pi,\mathbf{p}_{K^+})}{d\mathbf{p}_{K^+}}\right\rangle_j,\end{aligned}$$

[8] Such approximation, as showed our calculations, has a minor effect on the respective cross sections

$$\left\langle E_{K^+}\frac{d\sigma_{\pi^+n\to K^+X}(p_\pi,\mathbf{p}_{K^+})}{d\mathbf{p}_{K^+}}\right\rangle_j = \quad (92)$$
$$=\left\langle E_{K^+}\frac{d\sigma_{\pi^+n\to K^+\Lambda}(p_\pi,\mathbf{p}_{K^+})}{d\mathbf{p}_{K^+}}\right\rangle_j +$$
$$+\left\langle E_{K^+}\frac{d\sigma_{\pi^+n\to K^+\Sigma^0}(p_\pi,\mathbf{p}_{K^+})}{d\mathbf{p}_{K^+}}\right\rangle_j;$$
$$\left\langle E_{K^+}\frac{d\sigma_{\pi^0p\to K^+X}(p_\pi,\mathbf{p}_{K^+})}{d\mathbf{p}_{K^+}}\right\rangle_j = \quad (93)$$
$$=\left\langle E_{K^+}\frac{d\sigma_{\pi^0p\to K^+\Lambda}(p_\pi,\mathbf{p}_{K^+})}{d\mathbf{p}_{K^+}}\right\rangle_j +$$
$$+\left\langle E_{K^+}\frac{d\sigma_{\pi^0p\to K^+\Sigma^0}(p_\pi,\mathbf{p}_{K^+})}{d\mathbf{p}_{K^+}}\right\rangle_j,$$
$$\left\langle E_{K^+}\frac{d\sigma_{\pi^0n\to K^+X}(p_\pi,\mathbf{p}_{K^+})}{d\mathbf{p}_{K^+}}\right\rangle_j =$$
$$=\left\langle E_{K^+}\frac{d\sigma_{\pi^0n\to K^+\Sigma^-}(p_\pi,\mathbf{p}_{K^+})}{d\mathbf{p}_{K^+}}\right\rangle_j;$$
$$\left\langle E_{K^+}\frac{d\sigma_{\pi^-p\to K^+X}(p_\pi,\mathbf{p}_{K^+})}{d\mathbf{p}_{K^+}}\right\rangle_j =$$
$$=\left\langle E_{K^+}\frac{d\sigma_{\pi^-p\to K^+\Sigma^-}(p_\pi,\mathbf{p}_{K^+})}{d\mathbf{p}_{K^+}}\right\rangle_j,$$
$$\left\langle E_{K^+}\frac{d\sigma_{\pi^-n\to K^+X}(p_\pi,\mathbf{p}_{K^+})}{d\mathbf{p}_{K^+}}\right\rangle_j = 0. \quad (94)$$

Here:

$$\left\langle E_{K^+}\frac{d\sigma_{\pi N\to K^+Y}(p_\pi,\mathbf{p}_{K^+})}{d\mathbf{p}_{K^+}}\right\rangle_j = \iint P_j(\mathbf{p}_t',E')d\mathbf{p}_t'dE' \quad (95)$$
$$\times\left[E_{K^+}\frac{d\sigma_{\pi N\to K^+Y}(\sqrt{s_1},\mathbf{p}_{K^+})}{d\mathbf{p}_{K^+}}\right]$$
$$=\frac{\pi}{Q}\int dE'\int\limits_{p_t^-(E')}^{p_t^+(E')} p_t'dp_t'P_j(p_t',E')$$
$$\times\int\limits_0^{2\pi}d\varphi'\frac{1}{I_2[s_1(x_0,\varphi',E'),m_Y,m_K]}$$
$$\times\frac{d\sigma_{\pi N\to K^+Y}[s_1(x_0,\varphi',E')]}{d\overset{*}{\Omega}},$$

with

$$p_t^\pm(E')=|Q\pm\sqrt{(\omega+<E_t'>)^2-m_Y^2}|, \quad (96)$$

$$s_1(x,\varphi',E')=(E_\pi+<E_t'>)^2-p_\pi^2-p_t'^2 \quad (97)$$
$$-2p_\pi p_t'(\cos\vartheta_{\mathbf{Q}}\cdot x+\sin\vartheta_{\mathbf{Q}}\cdot\sqrt{1-x^2}\cos\varphi'),$$

$$x_0=\left[(\omega+<E_t'>)^2-m_Y^2-Q^2-p_t'^2\right]/(2Qp_t'), \quad (98)$$

$$Q=|p_\pi\boldsymbol{\Omega}_0-\mathbf{p}_{K^+}|,\ \cos\vartheta_{\mathbf{Q}}=\boldsymbol{\Omega}_0\mathbf{Q}/Q, \quad (99)$$
$$\sin\vartheta_{\mathbf{Q}}=\sqrt{1-\cos^2\vartheta_{\mathbf{Q}}}.$$

One can show that the expression for $I_V[A,\sigma_{pN}^{in}(p_0),<\sigma_{\pi N}^{tot}>,0^0]$ in the case of a nucleus of a radius $R=1.3A^{1/3}$ fm with a sharp boundary has the following simple form [38]:

$$I_V[A,\sigma_{pN}^{in}(p_0),<\sigma_{\pi N}^{tot}>,0^0]=\frac{9A^2}{2\pi R^2(a_2-a_3)} \quad (100)$$
$$\times\left\{\frac{1}{a_2^3}[1-(1+a_2)e^{-a_2}]-\frac{1}{a_3^3}[1-(1+a_3)e^{-a_3}]\right.$$
$$\left.-\frac{1}{2a_2}+\frac{1}{2a_3}\right\},$$

where $a_2=3\mu(p_0)/2\pi R^2$ and $a_3=3A<\sigma_{\pi N}^{tot}>/2\pi R^2$.

We have taken into account in the calculation of the K^+ production cross section (90) from the two–step processes (46)–(49) also the following medium effects[9]: the influence of the respective optical potentials on the incoming proton (denoted by V_0), on produced in the reactions (46), (47) nucleons (denoted by V_N) and (48), (49) hyperons (denoted by V_Y). The high–energy pion potential in a nuclear medium was set to zero [30–32, 35, 36]. In this case, as it is easily seen, one has to make the following substitutions in the formulas (7), (60), (68) and (71) for the quantities s, $p_\pi^{max}(\mathbf{p}_t,E)$, s_{NN} and $s_{NN\pi}$, respectively, which are involved in the description of the pion production processes (46), (47): $E_0\to E_0-V_0-2V_N$, $\mathbf{p}_0\to\mathbf{p}_0'$, where $\mathbf{p}_0'$ is the in–medium momentum of the initial proton ($p_0'^2=p_0^2-2m_NV_0-V_0^2$). And in the formulas (96)–(98) for the quantities $p_t^\pm(E')$, $s_1(x,\varphi',E')$ and x_0 involved in the description of the kaon production processes (48), (49) one has to replace the total pion energy E_π by $E_\pi-V_Y$. Consider now the specific values of the optical potentials V_0, V_N and V_Y used in our calculations. According to [3, 5, 51], a proton impinging on a nucleus at a bombarding energy of about $\epsilon_0\approx 1\ GeV$ feels inside the target nucleus the repulsive optical potential of about $V_0\approx 40\ MeV$. We have used this value of potential

[9] We have neglected the analogous medium effects in calculating the K^+ production cross section (3) in the one–step processes (1), (2), since the contribution from them to these processes is expected to be small in the subthreshold energy region where the participating target nucleons, unlike of the two–step production processes (46)–(49), need be far off–shell. It is fairly obvious that in the above threshold energy region the one–step kaon production processes (1), (2) are insensitive also to these medium effects because of relatively weak dependence of the corresponding elementary cross sections from energy in this region. Nevertheless, it would be interesting to carry out in the future a detail study of subthreshold kaon production in the one–step processes (1), (2) that includes consistently the medium effects under consideration

V_0 also at higher beam energies considered in the present work. Further, since the integration of (90) is exhausted within a relatively small range of p_π values below p_π^{max} at subthreshold incident energies, the relevant kinetic energy ϵ_N of each nucleon produced in the first interaction together with a pion with momentum in this range can be approximately estimated as: $\epsilon_N \approx (\epsilon_0 - \epsilon_\pi^{max} - m_\pi)/2$. Using the results for the maximum kinetic energy ϵ_π^{max} of a pion produced in the first pN collision, presented in Fig. 4, we readily get that $\epsilon_N \approx 0.1\ GeV$ at beam energies of $1.0 \div 1.5\ GeV$. Such low–energy outgoing nucleons feel in the interior of the nucleus the attractive optical potential $V_N \approx -(p_F^2/2m_N) + \epsilon_A$ [52], where p_F is the Fermi momentum and the quantity ϵ_A is defined above (see, (22)). Taking into account that $p_F = 221\ MeV/c$ [13] and $\epsilon_A = -7.0\ MeV$ [43] for C^{12} target nucleus, we obtain that $V_N \approx -33\ MeV$. In order to study the sensitivity of the kaon production cross section from the two–step processes (46)–(49) to the potential V_N, we have employed in our calculations also the value of $-50\ MeV$ [53] for V_N which is seen by nucleons near the top of the Fermi sea. Since at proton energies up to $1.5\ GeV$ hyperons from secondary πN collisions have a larger weight and due to kinematics are less energetic (their average kinetic energies are $\approx 0.2 \div 0.3\ GeV$ as it can be estimated from the results presented in Fig. 4) than those from primary pN collisions, it is naturally to use (see, also, [54]) for the optical potentials V_Λ and V_Σ seen by the final low–energy Λ and Σ hyperons the values of $V_\Lambda = -30\ MeV$ [53, 55] and $V_\Sigma = -26\ MeV$ [55], obtained from the study of the binding and decay of hypernuclei.

Now, let us discuss the results of our calculations in the framework of approach outlined above.

2.2 Two–Step K^+ production processes: results and discussion

The results of our calculations by (90)–(100) for the double differential cross sections for the production of K^+ mesons from secondary $\pi N \to K^+ Y$ channels at an angle of 40^0 in the interaction of protons with energies of 1.2, 1.5 and 2.5 GeV with C^{12} nuclei and the same experimental data [8] as in Fig. 3 are given in Figs. 5–7. It is seen from the Figures mentioned above that:

1) the two–step K^+ production mechanism clearly dominates at subthreshold beam energies considered here only if we adopt the assumption about the influence of the respective optical potentials on the two–step production processes (46)–(49) and it is of minor importance at 2.5 GeV proton beam energy at the laboratory kaon momenta $p_{lab} \leq 1\ GeV/c$, whereas at $p_{lab} > 1\ GeV/c$ the contributions from the two–step and one–step kaon production processes are comparable;
2) the difference between the calculations with allowance for the influence of the corresponding optical potentials on the two–step production processes (46)–(49) and without it increases with decreasing incident energy;

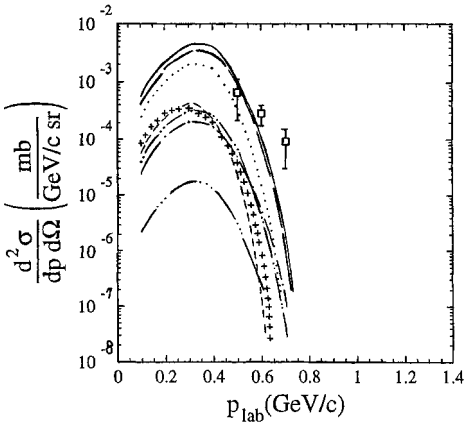

Fig. 5. Double differential cross section for the production of K^+ mesons at an angle of 40^0 in the interaction of protons of energy 1.2 GeV with C^{12} nuclei as a function of kaon momentum. The experimental data: [8]. The curves, our calculations: the *long–dashed line*, the *dashed lines with one*, *two* and *three dots* are calculations by (90)–(100) for the secondary production process (48) with $V_0 = 40\ MeV$ [3, 5, 51], $V_N = -50\ MeV$ [53], $V_\Lambda = -30\ MeV$ [53–55], respectively, for the use of uncorrelated part ($i = j = 0$), uncorrelated and correlated parts ($i = 0, j = 1$), correlated and uncorrelated parts ($i = 1, j = 0$), correlated part ($i = j = 1$) of the nucleon spectral function in the calculation of momentum–energy–averaged differential cross sections for pion and kaon production; the crosses are calculations by (90)–(100) for the secondary production process (49) with $V_0 = 40\ MeV$ [3, 5, 51], $V_N = -50\ MeV$ [53], $V_\Sigma = -26\ MeV$ [55] for the use of uncorrelated part of the nucleon spectral function in the calculation of momentum–energy–averaged differential cross sections for pion and kaon production; the *solid line* is the sum of the above curves and the results obtained by (3) for the one–step production channels (1), (2) (respective *light solid line* in Fig.3); the *dotted* and *short–dashed lines* denote the same as the *long–dashed line*, but it is supposed that $V_0 = 40\ MeV$, $V_N = -33\ MeV$ (see text), $V_\Lambda = -30\ MeV$ and $V_0 = 0$, $V_N = 0$, $V_\Lambda = 0$, respectively

3) the kaon yield is not very sensitive to the optical potential V_N that is seen inside the nucleus by nucleons produced in the first interaction together with an intermediate pion when this potential decreases from $V_N = -33\ MeV$ to $V_N = -50\ MeV$;
4) the main contribution to the K^+ production in the two–step reaction channels (46)–(49) both at subthreshold and above the free NN threshold incident energies considered here comes from the use only of the uncorrelated part $P_0(\mathbf{p}_t, E)$ of the nucleon spectral function in the calculation of the corresponding momentum–energy–averaged differential cross sections for pion and kaon production;
5) the K^+ production cross section in the two–step reaction channels (46)–(49) coming from the use of the uncorrelated and correlated parts of the nucleon spectral function in the calculation of momentum–energy–averaged differential cross sections for pion and kaon production, respectively, is approximately the same as

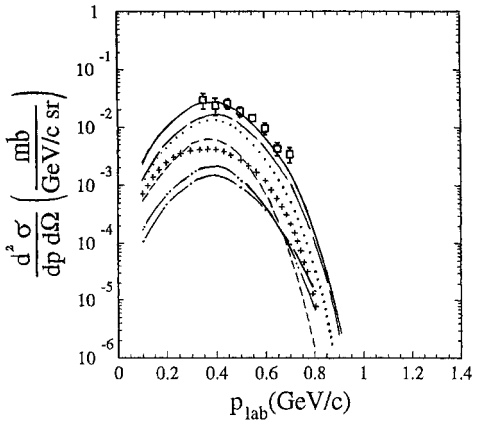

Fig. 6. The same as in Fig.5 but for 1.5 GeV beam energy

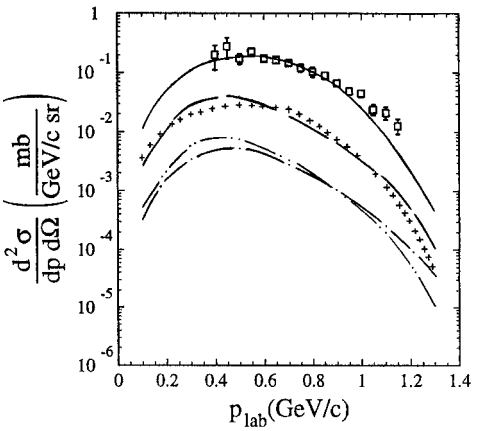

Fig. 7. The same as in Fig.5 but for 2.5 GeV beam energy

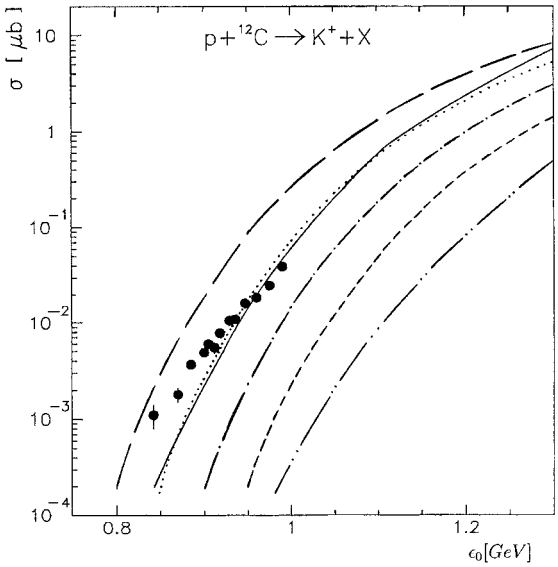

Fig. 8. The total cross section for K^+ production in $p + C^{12}$–reactions as function of the laboratory energy of the proton. The experimental data: [1]. The curves: calculations. The *long–dashed, dotted, dot–dashed* and *short–dashed lines* are our calculations by (90)–(100) for the secondary production process (48) with the use of uncorrelated part of the nucleon spectral function at $V_0 = 40\ MeV$, $V_N = -50\ MeV$, $V_\Lambda = -30\ MeV$; $V_0 = 40\ MeV$, $V_N = -33\ MeV$, $V_\Lambda = -30\ MeV$; $V_0 = 0$, $V_N = 0$, $V_\Lambda = -30\ MeV$ and $V_0 = 0$, $V_N = 0$, $V_\Lambda = 0$, respectively. The *dashed line with two dots* is calculation by (3)–(8), (13), (17) for the primary production processes $pN \to K^+\Lambda N$ with the use of the total nucleon spectral function. The *solid line* is the calculation for the two–step reaction mechanism within the spectral function approach [9]

that obtained from the use of the correlated and uncorrelated parts of one in the analogous calculation;

6) the contribution to the K^+ production in the same reaction channels only from the correlated part $P_1(\mathbf{p}_t, E)$ of the nucleon spectral function is an order of magnitude smaller than the contributions from the use of the uncorrelated (correlated) and correlated (uncorrelated) parts of one in calculating the momentum–energy–averaged differential cross sections for pion and kaon production, respectively;
7) the contributions to the K^+ production from the secondary reaction channels (48) and (49) with a Λ and a Σ particles in the final states are comparable at 2.5 GeV beam energy, whereas at subthreshold energies the secondary production process (48) is more important than the (49) one;
8) our full calculations (the sum of results obtained both for the one–step (1), (2) and two–step (46)–(49) reaction channels, solid lines) reproduce the experimental data only if we take into account the influence of the respective optical potentials on the two–step production processes (46)–(49).

Finally, in Fig. 8 we show the comparison of the results of our calculations by (90)–(100) for the total cross sections for K^+ production in pC^{12} collisions from secondary $\pi N \to K^+\Lambda$ channels with the use only of uncorrelated part of the nucleon spectral function as well as the same in–medium modifications of the corresponding quantities involved in the description of a pion and hyperon production as in above with the experimental data [1] and with calculations for the two–step reaction mechanism within the approach [9] with the total nucleon spectral function taken from [27]. In this Figure we also show the total cross sections for K^+ production from primary $pN \to K^+\Lambda N$ channels calculated according to (3)–(8), (13), (17) with the full nucleon spectral function. One can see that:

1) our model calculations with the set of parameters $V_0 = 40\ MeV$, $V_N = -33\ MeV$, $V_\Lambda = -30\ MeV$ (dotted line) that allows us to describe the existing experimental data [8] on the double differential kaon production cross sections reproduce also the measured [1] total K^+ production cross sections at proton energies above about 900 MeV but underestimate the data at lower bombarding energies, what indicates the need for other reaction channels or multinucleon correlations to explain these data close to the absolute production threshold;
2) the results of our calculations of the kaon yield from secondary $\pi N \to K^+\Lambda$ channels without employing the medium effects considered by us (short–dashed

line) underestimate essentially the data [1] and are larger only by a factor of 3–5 than those obtained for the one–step production channels, the latter is in line with our findings inferred above from the analysis of the data on double differential kaon production cross sections;

3) practically the same description of the data as our one was obtained also within the spectral function approach [9] (solid line) for the two–step reaction mechanism with an intermediate pion with employing only the repulsive impinging proton optical potential.

This can be probably attributed to the fact that different spectral functions have been used in the work presented here and in approach [9].

Taking into account the considered above, one may conclude that the high momentum and high removal energy part of the nucleon spectral function which is generated by ground–state two–nucleon short–range correlations apparently cannot be studied in the inclusive subthreshold and near threshold kaon production in pA reactions. As it was shown in [38], the $\pi^+ + A \to K^+ + X$ reaction in the subthreshold regime seems to be quite promising for this aim.

3 Summary

In this paper we have calculated the total and differential cross sections for K^+ production from $p + C^{12}$ reactions in the near threshold and subthreshold energy regimes by considering incoherent primary proton–nucleon and secondary pion–nucleon production processes within the framework of an appropriate folding model, which takes properly into account the struck target nucleon momentum and removal energy distribution. The comparison of the results of our calculations with the existing experimental data [1, 8] was made. It was found that the in–medium modifications of the available for pion and kaon production invariant energies squared due to the respective optical potentials are needed to account for the experimental data both from Koptev et al. [1] and from the SATURNE/GSI collaboration [8]. It was shown also that the two–step K^+ production mechanism clearly dominates at subthreshold energies considered here only if we take into account these modifications and it is of minor importance at 2.5 GeV proton beam energy at the laboratory kaon momenta $p_{lab} \leq 1\ GeV/c$, whereas in the region $p_{lab} > 1\ GeV/c$, where the kaon spectrum from the one–step K^+ production mechanism is entirely governed by the correlated part of the nucleon spectral function, the contributions from the two–step and one–step kaon production processes are comparable. Our investigations indicate that the main contribution to K^+ production in the secondary reaction channels comes from the use only of the uncorrelated part of the nucleon spectral function. Therefore, inclusive subthreshold and near threshold kaon production in pA collisions does not provide an information on the high momentum components within target nucleus.

One of us (E.Ya.P.) was supported in part by Grant No.96–02–19232 from the Russian Foundation for Fundamental Research.

References

1. Koptev, V.P., Mikirtyhyants, S.M., Nesterov, M.M., Tarasov, N.A., Shcherbakov, G.V., Abrosimov, N.K., Volchenkov, V.A, Gridnev, A.B., Yeliseyev, V.A., Ivanov, E.M., Kruglov, S.P., Malov, Yu.A., Ryabov, G.A.: ZhETF. **94**, 1 (1988)
2. Shor, A., Perez-Mendez, V., Ganezer, K.: Nucl. Phys. **A514**, 717 (1990)
3. Cassing, W., Batko, G., Mosel, U., Niita, K., Schult, O., Wolf, Gy.: Phys. Lett. **238B**, 25 (1990)
4. Sibirtsev, A.A., Büscher, M.: Z. Phys. **A347**, 191 (1994)
5. Cassing, W., Demski, T., Jarczyk, L., Kamys, B., Rudy, Z., Schult, O.W.B., Strzalkowski, A.: Z. Phys. **A349**, 77 (1994)
6. Sibirtsev, A.: Phys. Lett. **359B**, 29 (1995)
7. Müller, H., Sistemich, K.: Z. Phys. **A344**, 197 (1992)
8. Debowski, M., Grosse, E., Senger, P.: GSI Scientific Report, **10**, (1995); Debowski, M., Barth, R., Boivin, M., Le Bornec, Y., Cieslak, M., Comets, M.P., Courtat, P., Gacougnolle, R., Grosse, E., Kirchner, T., Martin, J.M., Miskowiec, D., Müntz, C., Schwab, E., Senger, P., Sturm, C., Tatischeff, B., Wagner, A., Walus, W., Willis, N., Wurzinger, R., Yonnet, J., Zghiche, A.: Z. Phys. **A356**, 313 (1996)
9. Sibirtsev, A., Cassing, W., Mosel, U.: LANL Preprint **Nucl–th/9607047** (1996)
10. Schult, O.W.B., Sistemich, K., Koptev, V., Müller, H., Cassing, W., Jarczyk, L., Komarov, V.I., Sibirtsev, A., Ernst, J.: Nucl. Phys. **A583**, 629 (1995)
11. Palmeri, A., Badala, A., Barbera, R., Bonasera, A., Ekstrom, C., Ericsson, G., Höistad, B., Johansson, T., Pappalardo, G.S., Riggi. F., Russo, A.C., Traneus, E., Turrisi, R., Westerberg, L.: CELSIUS Proposal, Uppsala (1994)
12. Geaga, J.V., Chessin, S.A., Grossiord, J.Y., Harris, J.W., Hendrie, D.L., Schroeder, L.S., Treuhaft, R.N., Van Bibber, K.: Phys. Rev Lett. **45**, 1993 (1980)
13. Frullani, S., Mougey, J.: Adv. Nucl. Phys. **14**, 1 (1984)
14. Pace, E., Salme, G.: Phys. Lett. **110B**, 411 (1982)
15. Ciofi degli Atti, C.: Nuovo Cimento. **76A**, 330 (1983)
16. Ciofi degli Atti, C., Liuti, S.: Phys. Lett. **225B**, 215 (1989)
17. Ciofi degli Atti, C., Liuti, S., Simula, S.: Phys. Rev. **C41**, R2474 (1990)
18. Ciofi degli Atti, C., Pace, E., Salme, G.: Phys. Rev. **C43**, 1155 (1991)
19. Ciofi degli Atti, C., Simula, S., Frankfurt, L.L., Strikman, M.I.: Phys. Rev. **C44**, R7 (1991)
20. Benhar, O., Fabrocini, A., Fantoni, S., Sick, I.: Nucl. Phys. **A579**, 493 (1994)
21. Ciofi degli Atti, C., Simula, S.: Phys. Rev. **C53**, 1689 (1996)
22. Ciofi degli Atti, C., Simula, S.: Phys. Lett. **319B**, 23 (1993)
23. Ciofi degli Atti, C., Simula, S.: Phys. Lett. **325B**, 276 (1994)
24. Weinstein, L.B., Warren, G.A.: Phys. Rev. **C50**, 350 (1994)
25. Akhiezer, A.I, Sitenko, A.G., Tartakovskii, V.K.: Nuclear Electrodynamics, **Springer–Verlag** (1994)

26. De Witt Huberts, P.K.A.: J.Phys. **G16**, 507 (1990)
27. Sick, I., Fantoni, S., Fabrocini, A., Benhar, O.: Phys. Lett. **323B**, 267 (1994)
28. Efremov, S.V., Paryev, E.Ya.: The 25th INS International Symposium on **"Nuclear and Particle Physics with High–Intensity Proton Accelerators".** Tokyo, Japan, December 3–6, 1996. Book of Abstracts and Contributed Papers, p.44–45
29. Efremov, S.V., Kazarnovsky, M.V., Paryev, E.Ya.: Z. Phys. **A344**, 181 (1992)
30. Fang, X.S., Ko, C.M., Zheng, Y.M.: Nucl. Phys. **A556**, 499 (1993)
31. Fang, X.S., Ko, C.M., Li, G.Q., Zheng, Y.M.: Nucl. Phys. **A575**, 766 (1994)
32. Fang, X.S., Ko, C.M., Li, G.Q., Zheng, Y.M.: Phys.Rev. **C49**, R608, (1994)
33. Randrup, J.: Phys. Lett. **99B**, 9 (1981)
34. Cugnon, J., Lombard, R.M.: Phys. Lett. **134B**, 392 (1984)
35. Li, G.Q., Ko, C.M., Li, Bao–An.: Phys. Rev Lett. **74**, 235 (1995)
36. Li, G.Q., Ko, C.M.: Nucl.Phys. **A594**, 460 (1995)
37. Li, G.Q., Ko, C.M.: Nucl.Phys. **A594**, 439 (1995)
38. Efremov, S.V., Paryev, E.Ya.: Z. Phys. **A354**, 219 (1996)
39. Balewski, J.T., Budzanowski, A., Dombrowski, H., Goodman, C., Grzonka, D., Haidenbauer, J., Hanhart, C., Jarczyk, L., Jochmann, M., Khoukaz, A., Kilian, K., Kohler, M., Kozela, A., Lister, T., Maier, R., Moskal, P., Oelert, W., Prasuhn, D., Quentmeier, C., Santo, R., Schepers, G., Seddik, U., Sefzick, T., Smyrski, J., Sokolowski, M., Strzalkowski, A., Wolke, M., Wustner, P.: Phys. Lett. **388B**, 859 (1996)
40. Randrup, J., Ko, C.M.: Nucl.Phys. **A343**, 519 (1980); **A411**, 537 (1983)
41. Schürmann, B., Zwerman, W.: Phys. Lett. **183B**, 31 (1987); Zwermann. W.: Mod. Phys. Lett. **A3**, 251 (1988)
42. Koltun, D.S.: Phys. Rev. **C9**, 484 (1974)
43. Benhar, O., Ciofi degli Atti, C., Liuti, S., Salme, G.: Phys. Lett. **177B**, 135 (1986)
44. Kester, L.J.H.M., Hesselink, W.H.A., Kalantar–Nayestanaki, N., Mitchell, J.H., Pellegrino, A., Jans, E., Konijn, J., Steijger, J.J.M., Visschers, J.L., Zondervan, A., Calarco, J.R., DeAngelis, D., Hersman, F.W., Kim, W., Bauer, Th.S., Kelder, M.W., Papandreou, Z., Ryckebusch, J., Ciofi degli Atti, C., Simula, S.: Phys. Lett. **344B**, 79 (1995)
45. Frankfurt, L., Strikman, M.I.: Phys. Rep. **76**, 215 (1981); **160**, 236 (1988)
46. Million, B.: Phys. Rev. **C40**, 2924 (1989)
47. Bystricky, J., La France, P., Lehar, F., Perrot, F., Siemiarczuk, T., Winternitz, P.: J.de Physique. **48**, 1901 (1987)
48. Cugnon, J., Lombard, R.M.: Nucl.Phys. **A422**, 635 (1984)
49. Tsushima, K., Huang, S.W., Faessler, A.: LANL Preprint **Nucl–th/9602005** (1996)
50. Flaminio, V, Moorhead, W.G., Morrison, D.R.O., Rivoire, N: Compilation of Cross–Sections: π^+ and π^- Induced Reactions. **CERN-HERA** 83–01, 1983
51. Li, G.Q., Ko, C.M.: Phys. Lett. **349B**, 405 (1995)
52. Iljinov, A.S., Kazarnovsky, M.V., Paryev, E.Ya.: Intermediate Energy Nuclear Physics. **CRC Press, Inc. Boca Raton**, 1994
53. Dalitz, R.H., Gal, A.: Phys. Lett. **64B**, 154 (1976)
54. Rudy, Z., Cassing, W., Demski, T., Jarczyk, L., Kamys, B., Schult, O.W.B., Strzalkowski, A.:Z. Phys. **A351**, 217 (1995)
55. Dover, C.B., Walker, G.E.: Phys. Rep. **89**, 1 (1982)